Report #1

Suggestions for revision or reasons for rejection (will be published if the paper is accepted for final publication)

General comments

First of all, I am glad to see the authors have put great effort into improving the (methods behind the) manuscript, partly based on my suggestions. My main point of concern was that their energy balance model did not allow for changes in incoming longwave radiation, surface temperature and albedo, with associated feedbacks. The authors have now extended their model to include all these processes, which makes the results more consistent and more convincing. Furthermore, they have clarified the model description and revised the section based on the NARR data, such that it is in line with the rest of the manuscript.

Due to these changes, the methods behind the manuscript have improved significantly. However, I still have some comments on the manuscript, as outlined below.

The most important is that the revised manuscript is considerably longer than the first version and I do not think this is an improvement in all places. For the model description, it was indeed necessary to include more detail. The Introduction has also increased in length. Although it reads smoothly, it is very long for an introduction and I suggest to make it more concise. The Discussion section has been rewritten completely. The present form reads like an evaluation of the results from the three different experiments grouped per perturbed variable. In my opinion, it is primarily a repetition of previously presented results with little discussion added. The last two paragraphs deal with suggested model improvements (without new subtitle...) and are more at place in a discussion section. On the other hand, some results are (also) discussed in the Conclusions section, which is also rather lengthy. I would suggest the authors to look critically at the Discussion and Conclusions sections and rewrite them. They should make sure that repetition is kept to a minimum and that no new discussion items are introduced in the Conclusions. Furthermore, they could perhaps address the representativity of their results for other parts of the glacier and shortly discuss the applicability of their methods on other glaciers.

Thanks to the reviewer for these suggestions. We rewrote much of the manuscript for the first re-submission, and it is true that parts of the discussion and conclusion were redundant. We have restructured the discussion and conclusion following the suggestions of both reviewers, and it is now shorter. Most of the 'summary' content in the discussion and conclusions that was covered in the results has been removed. The new content about insolation in the conclusions has been removed, and we bring in a little bit about glacier-wide applications in the discussion (ll. 970-985). The introduction has also been shortened by about 10%, but remains longer than the original submission in the interest of giving proper attention to some previous work on energy balance sensitivity studies.

The effect of the snowpack depth at the beginning of the melt season is now also investigated, which is definitely interesting. However, I am not convinced by the method used. It is not clear to me how the experiment is conducted, it seems like the model is only run for one year with averaged daily meteorological values (also mentioned below). The new figure (Fig. 7) shows small effects of initial snowpack depth for depths above 1.2 m w.e., but the values fluctuate around zero. I do not understand where this variability comes from, it seems random. Is it because snowfall events are prescribed randomly and would it not be better to keep the timing of snowfall events the same for all runs? Furthermore, I am a bit surprised by the low albedo prescribed for snow remaining all summer. It is only slightly larger than the ice albedo; whether the surface consists of snow or ice after day 220 makes little difference for the energy balance. Is this realistic?

This is useful feedback, and we are certainly open to ideas here. The reviewer is correct – we were running for only one year, using average daily weather conditions for the period 2002-2012. Our wish is to isolate the effects of the initial snowpack, so this seems like a sensible way to do this: repeat the same weather but for different initial (May 1) snow conditions. But it is true the averaging gives a weather time series that is not real. We now do this differently, running for the 11 years of actual weather but over the suite of initial snowpacks. In the end it does not change much, as we are averaging the final result for presentation.

Yes, the random element in these graphs comes from the summer snowfall events – they are an internal part of the code and we left this on through these experiments. This could be specified to control for this, to make the graph cleaner, although the process is separate from and independent of the winter snow extent so it is not systematically interfering with the experiment. It just gives some variability between realizations. We left this on, but comment on it and note that the summer snow gives 'internal variability' of about Q_N = 1 W/m^2, averaged over the summer (control experiments, not shown).

The final point, concerning the minimum snow albedo, is insightful and the reviewer is quite right that this 'old snow' value (0.3 for us) is very low and explains why the difference between exposed ice and old snow did not matter very much in the previous submission. Our number is based on observations from Haig Glacier firn, and our default treatment was to set the minimum snow albedo to that of firn. But this is may not be appropriate – firn on this glacier has an accumulation of impurities, similar to what occurs in ablation zones, so it is darker than old seasonal snow. Values of wet, impurity-rich, late-July snow at the AWS site on Haig are about 0.36. This may still be darker than values higher up in the glacier accumulation area, or at other glacier sites. To be a bit more 'typical' we set a new default value of 0.4 for the minimum snow albedo. All experiments in the paper now use this value. Figure 7c is new, showing the net energy sensitivity to winter mass balance for both α_{min} = 0.3 and 0.4. Results are indeed sensitive to this choice for the late-summer energy balance. As expected, higher values of α_{min} give a stronger influence of a deep winter snowpack, although the graph is still asymmetric – a shallow winter snowpack leads to large increases in summer melt, while a deep winter snowpack moderately reduces melt at this site. This result depends on how close one is to the ELA – lower on the glacier, the result would be reversed. This is discussed in the text.

Regarding the figures, I would strongly recommend the authors to add legends explaining the different lines/symbols. Every figure shows new variables, many with multiple lines. Determining the meaning of all lines from the (sometimes incorrect, see below) captions is complicated and unnecessary. Related to this, I would suggest to show a smaller variation of fluxes (with standard colours) to make the figures more consistent. For example, the turbulent fluxes are sometimes shown separately, sometimes combined and then in another figure combined with the subsurface heat flux.

This is a good suggestion – there is not always room to add legends, so we put this information in the captions and tried to stay consistent, but agreed that we have too many lines and colours, and it changes every plot. We now have legends for each figure, where applicable. We also simplified a bit, e.g. removed Q_C in Figure 3, and radiation and turbulent fluxes are now combined in Fig 6 to reduce the amount of information.

Where the figures are discussed in the text, the authors sometimes refer to the specific line colour in the text. This should be avoided, it should be easy to derive from the figures, by means of a legend. In general, the authors may try to refer less directly to the figures and tables, by only adding references in brackets and not in the main text.

Revised as suggested throughout the text.

Some detailed comments

16 (and elsewhere): The authors now investigate the effect of changes in winter snowpack depth. However, they refer to this variable as 'winter snowpack', while they should add a measurable quantity like 'depth' or 'thickness'.

Revised as suggested, l.16 and in Section 4 (discussion of Figure 7).

127-128: Positive net energy will not drive subsurface warming, as this has already been taken care of by Q_C.

Revised, l.112

133-134: If the unit is given for Eq. (3), the unit for Eq. (2) should also be given (W m-2), as one follows from the other.

Added, l.105

245: 'phi_t(z)'

Revised, l.231

249-260: How is the refreezing rate calculated?

We added a brief explanation on this, ll.234-238. In essence through an enthalpy model. If liquid water is present in the pore space and conductive cooling gives an energy deficit, the available ‘negative energy’ is diverted to latent heat of freezing; temperature are not allowed to cool in a layer until liquid water content $\theta w = 0$.

293: In what sense is the grid fixed, with respect to the surface or a reference layer? How are changes in snow depth and ice surface lowering incorporated? Are layers added/removed or is the grid shifted?

Good questions, we briefly explain this now, l.282 and ll.293-296. It is a fixed grid with respect to the surface, to a depth of 10 m (irregularly spaced, with nz=33). Near-surface layers are 10 cm thick. Snow depth d is modelled in a sort of Lagrangian sense, to the mm, so it is allowed to continuously accumulate, melt, or undergo densification (on a daily time step). Then at depth d below the surface, the grid cell has a weighted combination of thermal properties and densities to reflect the mixture of snow and either firn or ice in that layer. There is also a discrete step involved: every time 10 cm of snow accrues or ablates, the grid is shifted to propagate up/down the internal density/liquid water/ice layer structure. We hope this makes sense – happy to explain this further but we don’t want to go sideways in this paper on the details of the subsurface model. It probably needs to be described elsewhere in proper detail.

340-341: The reference to Eq. (11) is not correct.

Revised, l.330

355-356: Why is no aging included for summer snow events like for the seasonal snow pack?

It is, the clock starts again and albedo will decay. But this does not happen much as summer snows usually melt within 1-2 days. Clarified, l.346

360: I am a bit confused that internal melting can occur in this model. The main source would be penetration of solar radiation, but this is not included here. Where does the melt energy come from and is it a large term?

Quite right, there should be no internal melting since we don’t account for shortwave radiation penetration or meltwater/rainwater temperatures above 0°C. It is built into the code as an option (when we get to some attempt to include these processes), but is a ‘latent’ option right now. This statement has been removed, l.353.

442-449: The main reason to use JJA for the theoretical sensitivities is that the surface is at the melting point, as a good approximation. This is not mentioned here. Please also replace 'here' by 'in this section' or 'to calculate the theoretical sensitivity' to stress the contrast with 'the next section' with the 'modelled sensitivity', where the full melt season is considered.

True of course, now noted, l.433. Clarification on ll.444-447 for the second point.

679 (and Table 4): Not MJJAS melt energy as mentioned before?

No, we are trying our best to make it shorter and more focused where we can – so as of the first re-submission we now report only JJA, although we run the model year-round for the 11-year period (including May and Sept melt). The sensitivities in MJJAS are not so different from JJA, so we are sticking to that to increase the focus.

758-759: How is the energy balance model forced with this mean annual record? Do I understand it correctly that this record spans one year and has the mean value over the entire period for each day and each variable? This seems rather artificial to me, it does not represent real meteorological situations anymore. Why not run over the entire period using the same winter snow pack depth for each year per run?

Discussed above. It is true, averaging makes for an unrealistic time series in lots of ways, not too hot and not too cold. This can certainly be done as suggested, and it is consistent with the other perturbations (i.e. 11 realizations for each meteorological anomaly). We reworked this section thoroughly, starting at l.710.

789-793: Why are standard deviations not compared over the same period (2002-2012)?

That is a fair point, we are interested in the variability over the full NARR period, 1979-2014, but it is probably not appropriate to compare those numbers to the 11 years of observation. We revised this to report the NARR variances over the common period, 2002-2012, ll.761-764. Values did not change much.

1021: Refreezing of melt water acts as an energy source (not sink) through release of latent heat.

Thanks yes, this was loose language. We were thinking of the energy sink as the positive net energy that is required to re-melt refrozen meltwater. At night when there is sometimes refreezing, the energy that is released is often dissipated (e.g., as QC to the surface, LW emissions, etc). Then the next day new energy is required to melt some 'recycled' meltwater (the overnight ice crust). This text has been removed as part of the discussion rewrite.

759-760: The range is 0.35-2.35 in the caption of Fig. 7.

Revised, we ran in the end for 0.36-2.36 (the observed mean, 1.36, \pm 1)

Fig. 2b: As also suggested before: Either note that KG indicates Kwadacha Glacier, which is mentioned once in the paper or remove the dot and zoom in on the map around Haig Glacier. I suggest to do the latter.

Revised as suggested

Fig. 3: Better show net shortwave and net longwave radiation instead of incoming shortwave radiation and net radiation, then all fluxes are shown exactly once. I would also suggest to use a long horizontal axis for both plots and show them above/below each other instead of next to each other. Then the interannual variation is more clearly visible and corresponding days can be compared.

These are good suggestions, adopted. QC is also removed.

Fig. 6: Net radiation is mentioned twice in the caption.

The black line is net energy, thank you for noticing, it is revised now.

Figs. 9 and 10: Numbering of the figures is incorrect, the numbers are still from the previous manuscript.

Apologies, amended. These figures were not meant to be included – we removed this part of the analysis and discussion in the first revision, but the figures lingered.

Fig. 10: Why are the turbulent fluxes both underestimated with the NARR forcing? The meteorological variables show good correspondence...

These figures and the associated results are no longer discussed, as we chose to focus just on the sensitivities. But for the reviewer's interest, this problem went away with the revised code – it was because we were assuming a melting surface in the initial submission. Now that Ts is internally modelled with the subsurface temperatures, the modelled turbulent fluxes are much improved. But no longer discussed….

Report #2

Referee review for manuscript tc-2016-06-manuscript-version-3, submitted for publication in The Cryosphere

"Surface Energy Balance Sensitivity to Meteorological Variability on Haig Glacier, Canadian Rocky Mountains" by S. Ebrahimi and S. J. Marshall

General Comments

The revised manuscript is an improvement on the initial submission. In particular, the model now includes more dynamic feedbacks which has increased the confidence with which the results can be interpreted. The re-setting of the NARR results as an extension of the sensitivity analysis is good to see and improves the focus of the paper. The authors appear to have considered and addressed the main points in their response to my first review. However, it was difficult to assess the actual changes made to address each point as no text changes were given in the response and a marked up version of the manuscript was not supplied.

Apologies, the overall was so large that we did not quote specific revisions or invoke 'track changes'. The first draft was almost completely written in accord with the reviewers' suggestions, so this did not seem productive. In our second round of revisions, we use track-changes mode and the specific changes can be seen – still very extensive in the rewritten discussion, but possible to examine specifically through the rest of the text.

Also, the paper still contains many ambiguities of method and much inference that isn't always supported by robust results. The main result appears to be an extremely large increase in temperature sensitivity when albedo is allowed to vary. While one would expect the sensitivity to increase, the magnitude of the increase here needs to be better supported by the validation of the albedo scheme against measurements and further discussion or analysis around the role of impurities to justify the low minimum value for snow albedo used. The choice of minimum values of albedo for snow and ice also impacts the conclusion that winter balance is of less importance, as with higher minimum albedo values the contrast between snow and ice is larger and this will increase the sensitivity. The authors also need to comment on the processes driving this sensitivity - to what extent the sensitivity is driven by decreases in snow albedo, earlier transition to ice and summer snowfall.

The temperature sensitivity with albedo feedbacks is still high, doubling the response, but it is much reduced with the various model changes that went into the revisions. Now it is well in line with previous literature. We made numerous changes, but mostly we now introduce all parameterizations for consistency, in particular cloud feedbacks (via the clearness index), such that shortwave radiation decreases with increased humidity (more cloud), offsetting the increase in longwave radiation. This and the increase in minimum snow albedo to 0.4 have reduced the sensitivity. With the revised experiments, the only difference is temperature forcing with and without albedo feedbacks, i.e., the other temperature feedbacks such as length of the melt season, rain vs. snow, are the same in all temperature experiments (cases 1-4 in Table 4).

The use of parameterisation for the radiative fluxes that responds to various drivers is encouraging. There is still a need for a validation of the melt produced by the fully parameterised model against that driven with measurements if the results are to be trusted. It is also ambiguous which version of the model is being used for any particular run and this needs to be carefully detailed and explained.

We had not brought in a discussion of the energy balance and subsurface model performance and validation vs. observations or a 'reference' model, mostly because these models are based on Marshall (2014) and Ebrahimi and Marshall (2015), for the longwave parameterization, and the current paper is already long. We could spend some time on a model validation section, but fear that this would be a diversion. The reviewer is correct though, confirmation that the parameterized daily model gives a good representation of the summer energy balance and melt is needed in order to trust the results. We added two paragraphs on this (Section 3, ll.407-423).

The new text gives a summary of the parameterized model performance in a sample dataset from summer, 2015, for which the melt model was not tuned or calibrated. We observed/measured a total summer melt of 3.1 ± 0.1 m w.e. at the AWS site from May to September, 2015, based on a May snowpit (measured snow water equivalent), the AWS SR50 record, and ablation stake data. The energy balance and susbsurface snow temperature/ drainage model are run in two modes, forced by the 30-minute AWS data (best case or reference model) and with the parameterized model, that degrades the AWS data to daily forcing with parameterized albedo (Eq. 20), incoming longwave radiation (Eq. 8), and diurnal cycles of temperature and shortwave radiation from Eqs. (17) and (18). The reference model that is driven by 30-minute AWS data gives a total summer melt of 3.04 m w.e., and the parameterized daily model gives 2.98 m w.e., with a small under-prediction of melt due to over-estimated summer albedo values (figure R1). The RMS error in daily melt totals is 3% (0.7 mm, relative to a mean summer melt value of 23 mm w.e.). Daily melt predictions from each model are shown here:

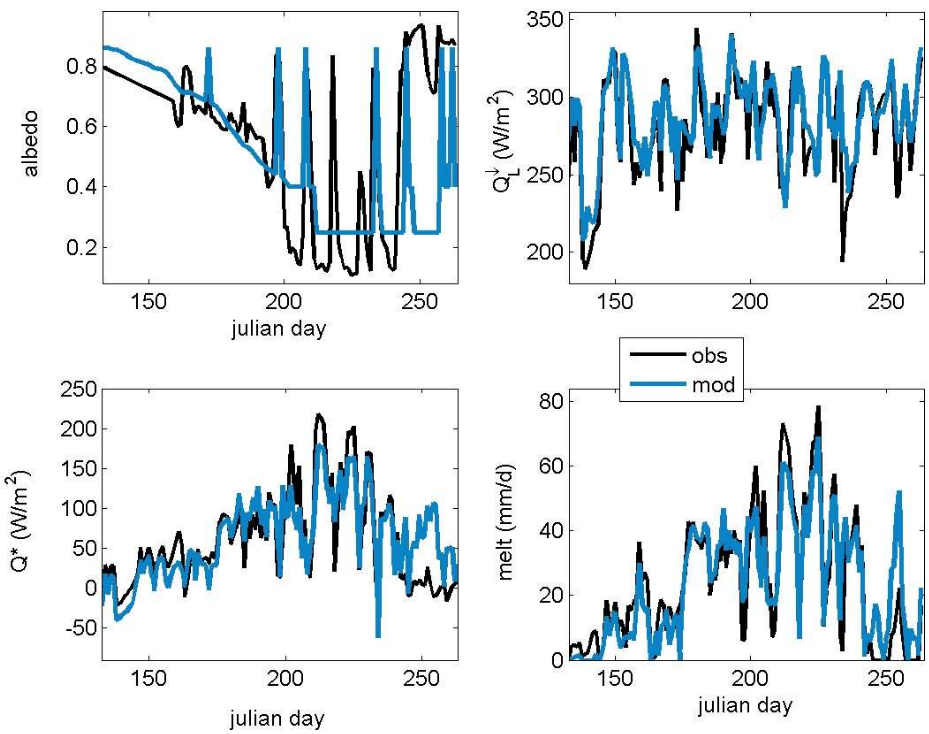

Figure R1. Parameterized model performance (blue) vs. the reference model (black), that is driven by 30-minute AWS data. There can be large departures in the melt daily melt rates (lower right), mostly attributable to discrepancies between the measured and modelled albedo (top left). The model overestimates albedo in summer 2015 (May-August) and underestimates it in September, when new snow (an early start of winter) is not adequately captured. Note that the downward-looking shortwave radiometer was not properly wired in summer 2015 from May 12-June 6 (day 133-157), so albedo is estimated for this portion of the record. Bare-ice albedo at the AWS site was close to 0.1 in summer 2015, but is not always this dark.

--

We do not include this figure or other model calibration discussions in the main text, as we don't want to lengthen it or take a tangent, but we summarize these statistics on model performance to address the question of whether model skill is adequate for the sensitivity analyses that are our main focus. This is just one summer, but the model was tuned for the period 2002-2012 and the performance is similar here; it is not perfect, especially for the albedo, but we believe the parameterized model has reasonable skill and is a reliable tool for our present purpose.

The authors identify a series of significant feedbacks between air temperature, humidity and the incoming fluxes of short and longwave radiation. It would appear most of these are all connected through cloud cover, and it would be much clearer and insightful for the authors to explicitly examine changes in the frequency and attenuation of cloud cover alongside with air temperature and humidity, rather than inferring these from the sensitivity of incoming shortwave radiation in the analysis of the in-situ dataset. This should be possible as the authors already have a parameterisation of cloud cover that includes humidity. If not, then the variability in incoming longwave also needs to be included in Table 4.

This is a good point and suggestion. We have rerun everything for the revised submission, with a simplified (identical) set of model parameterizations in all runs and with consistency of the shortwave and longwave radiation perturbations, through the transmissivity \tau. This is effectively our cloud proxy, and is now described as such. So we perturb \tau (\pm 0.1) and describe this as changes in cloud cover, which have opposite influences on incoming LW and SW radiation. Table 4 includes this now. Also, all experiments with a change in humidity see a corresponding change in \tau, hence incoming SW and LW. This is now internally consistent.

Moreover, all sensitivity studies in section 5 now use the parameterized version of the code, in the daily energy balance/subsurface temperature model. That is to say, we do not use the raw 30-minute AWS data to force the model, but rather the parameterized diurnal cycle, albedo model, modelled surface temperature, parameterized incoming longwave radiation, and parameterized clearness index (shortwave transmissivity), \tau. This allows clear understanding of our experiments and comparability across results. All of our numbers in Table 4 are revised as a result of these changes. Most have not changed much, but the temperature sensitivity with feedbacks is now much less – now more in line with observations and the NARR results.

In general, the paper is fairly well written though some of the text in the results and discussion is quite methodological and repetitive and perhaps is better suited to a methods section. Further work is needed to distill the main results from a rather large body of work and succinctly present them here.

Agreed, our results and discussion were repetitive and we did not do a good job of distilling the main results. We have rewritten and shortened this. We did keep some of the methodological details within the results, e.g., the details concerning the NARR forcing in section 6. The paper covers a lot, and we initially had much of this material in section 2 (methods), but it was far removed from the eventual results or NARR experiments and made for difficult flow/reading. The same holds true for the partial derivatives/theoretical sensitivities in Section 4. They are tiresome but are relevant locally (section 4) and not in the other results' sections. Hence we choose to combine methods and results to some degree in Sections 4-6, where specific to that section. We did our best to clean up the discussion, however.

The authors have managed to refocus their analysis but the new results and novelty of their results are often quite hidden. I would suggest re framing the discussion around 1. A summary of the important sensitivities and feedbacks that are observed on the Haig, 2. A discussion of the utility of the theoretical sensitivity based on mean summer conditions (good correspondence with full summers when feedbacks are omitted) 3. A discussion of the utility of exploring sensitivity to inter-annual variability with reanalysis datasets (mixed results). This structure would alert the reader to what is new and avoid some of the repetition.

The discussion and conclusion have been rewritten, somewhat but not fully along the lines suggested. We hope that the main results are now more clearly presented.

Line comments

204 - replace ‘profile method’ with ‘bulk aerodynamic method’. The profile method uses wind speeds and temperature at two heights.

Revised, l.187.

244 - the symbol psi has a different case from the equation.

Revised, l.227.

249 - please include an explanation of how the refreezing rate is calculated and what constraints are put on the volumetric water content.

Added as per request of both reviewers, ll.234-238 and ll.248-251. The upper constraint on the volumetric water content is the porosity of the snow or firn, but drainage in the seasonal snow is efficient enough that this is never approached; tracking θw evolution through the summer, it reaches a maximum of about 10%. There is a minimum (irreducible) water content in temperate snow, associated with capillary pressure, which we set to 3%.

278 - for consistency please state the model uses a variable timestep from 10 minutes to 1 hour to allow for stability of the subsurface temperature prognosis.

Revised as suggested, ll. 271-272.

349 - the minimum value for snow is very low. For the same site, Marshall (2014) gives 0.4 as a minimum. This will have a large impact on the sensitivity. Other authors have used values around 0.5 (Oerlemenas and Knap, 1998) and further justification of this low value is needed.

This is well observed, and R1 also questioned this. As discussed in the response to R1, this does of course impact the sensitivity; we now include experiments with both 0.3 and 0.4 as the minimum snow albedo (Figure 7), and have reverted to 0.4 as the default for the sensitivity studies (l.340). We initially used 0.3 because our observations at Haig Glacier indicate a value of 0.3 for firn, but old seasonal snow is closer to 0.4 at our site (see, e.g., the black line in Fig R1 above, just before the glacier ice is exposed). We sometimes see values below 0.4 for old snow at the Haig Glacier AWS site, in late summer, but 0.3 is probably too low to be representative of the accumulation area or the region, in general. It was our oversight to treat aged seasonal snow as firn; the latter has had more time to accumulate impurities.

405 - need to provide more discussion and evidence for the reasons for the decrease in albedo - i.e. is the increase in particulate concentrations documented?

The increase in particulate concentration is certainly observed, both in old snow and exposed firn and ice, but has never been quantified or supported by measurements. Empirically though, the seasonal albedo decrease at this site is strong, as has been documented elsewhere and as evident in e.g. Fig. R1 and Fig. 4a. Also see Fig. R2 below, for the average summer albedo evolution from 2002-2012. We assume that the seasonal decline is due to the water content, impurities, and grain growth in the temperate summer snowpack (after the conventional wisdom in Cuffey and Paterson and elsewhere), but it is fair to say that we are speculating as we don’t have measurements or process studies to attribute the causes of the seasonal albedo decrease. We just observe a snow albedo decline from ~0.8 to ~0.4 each summer, before it drops to ~0.2 on the bare ice (Fig. R2). A detailed study of this may be warranted, but is out of scope here. For now, we modify the text (ll.394-398) to note the observations and empirical record but stop short of attributing cause.

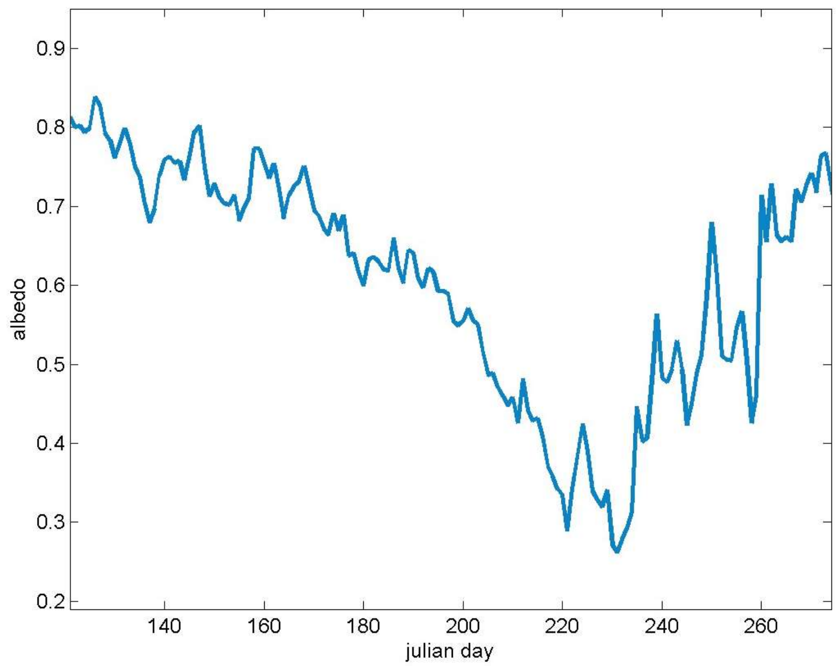

Figure R2. Average summer albedo evolution at the AWS site, 2002-2012.

419 - the contribution to melt should really be computed for melting periods only, as non-melting periods will bias these fractions towards the sensible heat flux (see Conway and Cullen, 2016). Please either show the fluxes for melting periods only or discuss only the contribution to the energy balance and not to melt.

Point taken, we now refer just to the contribution to the energy balance, l.404.

423-430 - please make it clear that the feedbacks and NARR analyses are presented in the following two sections, rather than the current section.

Revised; the NARR discussion has been removed from here as it was evidently distracting.

434 and 439 - some more context is needed to justify conditions on the Haig being 'typical' of other mid-latitude glaciers. Please add either a table showing this or some references to papers with similar climatologies.

This is fair; we suspect but cannot substantiate that all of the weather conditions here are ‘typical’ of mid-latitude glaciers. For instance, the elevation (hence pressure and vapour pressure) are lower than for glacier in the Alps and higher than the ablation zone of coastal mid-latitude glaciers; winds at other sites are often stronger than here; etc., etc. It is difficult to argue that mean conditions here are typical, and that is a loose qualitative word. In the end we removed this line and a bit of text around it from the manuscript, near l.430.

444 - need further analysis in order to justify that the JJA has more impact on melt? Table 3 shows an almost identical combined sensitivity.

Yes, it is true in the results – this is why we report it, as we did not necessarily expect MJJAS sensitivity to be the same. But JJA conditions have more impact on melt simply because 80% of the melt occurs in these months. A cold May or Sept does not have the same impact on summer mass balance as a cold July. Net energy sensitivities may not change much, but the impact on melt does. In any case, this is now N/A as the MJJAS sensitivities are no longer reported, at the reviewer's request (see below).

442-448 - this is quite a confusing paragraph as the rationale for including/excluding months changes from the start to the end of the paragraph and results are introduced, but not referenced properly. Please either point to the figures/tables that justify these statements or move this text to the discussion.

Paragraph has been revised and simplified, ll.444-447, sorry for the confusion.

453 - Are these perturbations calculated as the average of positive and negative deviations from the mean? Some of the text (e.g. 518) seems to suggest that only positive perturbations were considered, which is not ideal.

This is a bit interesting. Yes, in Section 5, with anomalies introduced into the numerical model, perturbations are always introduced as positive and negative deviations from the mean. Here where we consider theoretical sensitivities, the values are based on derivatives at a point (the mean state), so sensitivities can be considered to apply only at this point, i.e. for infinitesimal negative or positive perturbations from the mean. The result is the same for either sign of perturbation, as it is essentially the slope at the point. If the relationship is nonlinear, it becomes invalid for large negative or positive perturbations.

503 - I am not sure at this stage it is appropriate to transfer the calculations of net energy to melt, as in reality not all periods will have melting conditions. Perhaps it is better to state the increase or decrease in the net energy available. Along with this I would remove the melt column from table 3.

We agree, of course, and transfer the net energy perturbation to melt with a cautionary note (ll.504-508), but have retained this in Table 3 and the discussion because melt rates give a more intuitive idea of the potential impact, or lack thereof. The values can also be compared across the different perturbations. Moreover, JJA mean Q_N translates well to JJA melt at the site; the reference value is 97 W/m^2, which gives 2.30 m w.e. melt if this is converted directly to melting. The reference JJA melt is 2.32 m w.e. (Table 2), so within 1%.

516 - please be consistent with the symbols used - the text uses vapour pressure while table 3 shows specific humidity.

Revised, specific humidity throughout now, for the perturbations

604 - Please be explicit this is top of atmosphere solar variability.

This subsection has been rewritten, hopefully clear now.

620 - For comparing the relative importance of each variable - it would be more useful to present the individual sensitivities relative to 1 standard deviation perturbations in Table 3. Agreed – we have added the individual sensitivities to 1-σ perturbations and written this into the results. This also facilitates comparisons with Table 4 (modelled sensitivities).

630 - The way these variables have been perturbed is not meaningful as they are physically unrealistic. For example - some of the standard deviation in vapour pressure will be due to increases in relative humidity, but you also increase incoming shortwave in this experiment - which as you noted earlier is likely to decrease with increased relative humidity. Thus, the experiment is contradictory. Please exclude these last two lines in Table 3.

This is a fair point, we agree that it is inconsistent for all variables to change in the same sense. This was meant only to explore joint variability of multiple weather variables, as occurs in reality, but as implemented this was not meaningful. These two lines have been removed. It is better to explore meteorologically-meaningful covariability through NARR (section 6) or another means.

677 - It is still ambiguous which variables are held constant at their measured values and which are parameterised for each run (in particular incoming longwave and surface temperature). Please provide a comprehensive table.

We have clarified this in our numerical experiments and in the text. We now use the parameterized daily model for all experiments that we present; LW radiation, albedo, and surface temperature are all parameterized/internally calculated. The introduction hopefully clarifies this, ll.627-634.

680 - why were changes in incoming longwave not examined?

We now perturb the clearness index \tau, which jointly impacts incoming SW and LW radiation; experiments on the radiation fluxes are not considered. This is consistent with our effort to perturb observable weather variables (e.g., T, v, qv, clouds), and allows a sensible (albeit parameterized) co-variation of the incoming radiation fluxes.

764 - this result is likely to be strongly dependent on the choice of the minimum albedo of snow, which in this case does not differ much from an ice albedo. Either the sensitivity of this result should be tested, or a more thorough justification made for the very low value chosen here. (0.3)

Agreed and revised, as discussed above in some depth. The default minimum albedo is now 0.4, and Fig. 7c includes an illustration and brief discussion of the sensitivity to this parameter.

776 - are the anomalies calculated with respect to the mean in-situ conditions? I suspect you took the daily anomalies of NARR from the NARR climatology, then applied these daily anomalies to the mean in-situ conditions - please clarify.

Yes, this is correct. Clarified, l.751.

792 - it would be useful to see the standard deviation of relative humidity included here.

We don't actually use NARR relative humidity; it is derived from the specific humidity and temperature, for thermodynamic consistency. Hence any errors and variability in RH will flow from the NARR-derived T and qv. But for interest, the NARR RH is 65 \pm 3% (sigma = 2.8%).

801 - this line needs more context to link it with the previous sentences.

Revised, l.781.

970 - do the interannual anomalies in SWin and LWin from NARR correlate with the anomalies from the in-situ dataset? If not, it is hard to see how the NARR represents realistic interannual variability in these fluxes. This severely limits the inferences that can be made from model runs made with these anomalies.

We more or less agree – these are only weakly correlated, 0.52 for incoming SW radiation and 0.17 for incoming LW. Variables like temperature are much stronger (0.81). These are for only 11 years of mean JJA conditions, so the data is a bit limited. In summary, incoming SW is OK and incoming LW is very weak in the reanalysis. We note that NARR does not represent realistic interannual variability in these fluxes (l.765, l.779). Noted again in the discussion.

1005 - this statement needs more justification. It would seem that the NARR based reconstructions performed satisfactorily in describing interannual variations in net energy flux, but that this is based on the accidental cancelation of errors in the radiative fluxes driving the model (Figures 5 and 6 from the original manuscript. The approach is worthy of further exploration, but a more thorough evaluation of the performance of the model, including biases and areas for improvement, is needed here.

Yes, agreed, this is still the case that further work is needed if one wishes to drive glacier mass balance reconstructions with NARR forcing. We deliberately stopped short of that here, and revised the discussion to stay within the sensitivity study and recommend further work, as per the reviewer's suggestion.

1413 - needs a legend describing the colours. Also, box 4 could be better as a separate figure, as the colours indicate the change in Qn due to different forcing, while in the other boxes the colours show the response of different fluxes to the same forcing.

Legend now added and the figure has been simplified to show the same fluxes in each case.

1415 - both black and red are listed as net radiation - please fix.

Revised.

1416 - add 'please note the different y scales'.

Revised as suggested.

1416 - please clarify in the caption which scenarios these figures relate to in Table 4.

Revised as suggested.

1277 - net melt has decreased 7-8% while net energy fluxes have remained similar. It would be useful to show the fraction of time the surface is diagnosed as melting in each month to provide some justification here.

We no longer discuss the M-S conditions, to shorten and focus the ms. Agree though that this is interesting.

1388 - I am not sure this figure adds much as you cannot see the detail in the daily values over the 11-year period, and the results presented in the figure are not discussed in the text. I would suggest either removing the figure, or modifying the figure so it is readable and discussing the results further. If the figure is kept the size of each box needs to be expanded and the line weight reduced to make a more readable figure.

Figure has been modified to better illustrate the data. It is meant to give a sense of the observed/driving data. It is now discussed a bit more in the main text, ll.383-387

1394 - please use thinner lines on these figures. Also, as months and not day of year are discussed in the text, it would be good to have months as the x-axis label, or at the very least, further tick marks that are at monthly or 30 day intervals.

On panel d, the median + interquartile range would better present the seasonal variation of melt rate. As it is, the mean appears to be greatly influenced by individual large melt events (such as around day 230).

Revised as suggested, also panel d (now median and interquartile range). It is true in the early spring or late fall, the mean is influenced by large events, though not so much in JJA.

1430 - the y axis of figure 7a should be m w.e. in line with the text and Figure 7c.

Revised as suggested

1469 - 1495 - were these figures meant to be included?

Our mistake, apologies. Remnants of the first submission.

Surface Energy Balance Sensitivity to Meteorological Variability on Haig Glacier, Canadian Rocky Mountains

S. Ebrahimi and S. J. Marshall

Department of Geography, University of Calgary, 2500 University Drive, NW, Calgary, Alberta T2N 1N4, Canada

Correspondence to: S. Ebrahimi (samaneh.ebrahimi@ucalgary.ca)

Abstract

Energy exchanges between the atmosphere and the glacier surface control the net energy available for snow and ice melt. This paper explores the response of a mid-latitude glacier in the Canadian Rocky Mountains to daily and interannual variations in the meteorological parameters that govern the surface energy balance. We use an energy balance model to run sensitivity tests to perturbations in temperature, specific humidity, wind speed, incoming shortwave radiation, glacier surface albedo, and winter snowpack depth. Variables are perturbed (i) in isolation, (ii) including internal feedbacks, and (iii) with co-evolution of meteorological perturbations, derived from the North American regional climate reanalysis (NARR) over the period 1979-2014. Summer melt at this site has the strongest sensitivity to interannual variations in temperature, albedo, and ~~incoming shortwave radiation (i.e., cloud cover). Fluctuations in~~ specific humidity~~ also impact summer melt extent~~, while ~~interannual variability in~~ fluctuations in cloud cover, wind speed, and winter snowpack depth have less influence. Feedbacks to temperature forcing, in particular summer albedo evolution, ~~strongly amplify~~double the melt sensitivity to a temperature change. When meteorological perturbations co-vary through the NARR forcing, summer temperature anomalies remain important in driving interannual summer energy balance and melt variability, but they are reduced in importance relative to an isolated temperature forcing. Covariation of other variables (e.g., clear skies, giving reduced incoming longwave radiation) may be partially compensating for the increase in temperature. The methods introduced in this paper provide a framework that can be ~~adapted~~extended to compare the sensitivity of glaciers in different climate regimes, e.g., polar, maritime, or tropical environments, and to assess the importance of different meteorological parameters in different regions.

1. Introduction

Glaciers and icefields are thinning and retreating in all of the world's mountain regions in response to global climate change (e.g., Marzeion et al., 2014). This is reshaping alpine environments, affecting regional water resources, and contributing to global sea level rise (e.g., Radić and Hock, 2011). ~~Melting of glaciers has drawn great attention, and it is important to understand the meteorological controls of snow and ice melt to correctly project glacier response to climate variability and change.~~

A glacier's climate sensitivity can be expressed in terms of the energy or mass balance response to a change in meteorological conditions (Oerlemans and Fortuin, 1992; Oerlemans et al., 1998). ~~In a study of 12 glaciers by~~For instance, Oerlemans et al. (1998~~),~~) defined the static ~~or fixed-geometry~~glacier sensitivity to temperature, S_T, ~~is expressed~~i as:

$$S_T = \frac{\partial B_m}{\partial T} \approx \frac{B_m\,(+1K) - B_m\,(-1K)}{2} \qquad (1)$$

where $B_m(\delta T)$ denotes the mean specific mass balance corresponding to the temperature perturbation δT. Mass balance sensitivity to precipitation perturbations, $S_P = \partial B_m/\partial P$, ~~is~~can be calculated in the same way.

Braithwaite and Raper (2002) extended the static sensitivity approach to regional scales, with the idea that glaciers within a given climate regime should have similar mass balance sensitivities to variations in temperature and precipitation. This framework has been used in numerous studies to describe glacier sensitivity to climate change (e.g., Dyurgerov 2001; Klok and Oerlemans, 2004; Arendt et al., 2009; Anderson et al., 2010; Engelhardt et al., 2015). ~~Oerlemans et al. (1998) and Oerlemans (2005) also introduced measures of dynamic sensitivity, characterizing glacier volume and length changes as a function of changes in temperature.~~

Most studies to date have concentrated on glacier mass balance response to changes in temperature and precipitation. This is sensible, as these ~~two fields~~ are ~~perhaps~~generally the most important meteorological ~~parameters~~variables affecting glacier mass balance. ~~Temperature and precipitation~~These two fields are also commonly measured, with long-term records available in ~~some~~many regions~~, and extensive effort has gone into modelling and downscaling these two fields for a wide range of climate change impacts studies, including glacier modelling. Related to this,~~. Temperature and precipitation have also received the most attention because regional- to global-scale models of glacier mass balance commonly employ temperature-index methods to parameterize glacier melt (e.g., Marzeion et al., 2014; Clarke et al., 2015~~). This is appealing because temperature index models require only temperature and precipitation~~), with only these variables as inputs.

~~Temperature~~ While temperature index ~~methods~~models have ~~been~~ demonstrated ~~to have~~ reasonable skill in estimating seasonal melt (Ohmura, 2001; Hock, 2005), ~~but~~ they are nonetheless missing much of the physics that govern ~~snow and ice~~ melt. ~~Because temperature-index models estimate snow and ice melt as a function of air temperature, these models~~Also, they may be overly sensitive to changes in temperature, ~~and may not~~without effectively ~~capture~~capturing the impact of shifts in other ~~climate~~ variables such as wind, humidity, or cloud cover. Internal processes and feedbacks ~~that are important to glacier melt may also be absent,~~, such as ~~the~~ surface albedo evolution ~~that is~~

Formatted: Font color: Auto

Formatted: Font color: Auto

~~observed on glaciers during the melt season~~ , may also be absent, since degree-day melt factors are usually taken to be static. Such feedbacks are critical to glacier melt (e.g., Brock et al., 2000; Klok and Oerlemans, 2004; Cuffey and Paterson, 2010).

It is uncertain whether variability in glaciometeorological variables other than temperature and precipitation is important to glacier energy and mass balance. While most large-scale glacier change projections are rooted in temperature sensitivity (as built into temperature-index models), it is generally recognized that the complete surface energy balance is important to glacier melt ~~and its sensitivity to climate change.~~. For instance, net radiation has been identified as the main source of melt energy for continental glaciers, accounting for ~70-80% of the total melt energy (e.g., Greuell and Smeets, 2001; Oerlemans and Klok, 2002; Klok et al., 2005; Giesen et al., 2008~~;~~ ~~Marshall, 2014~~), with shortwave radiation providing the principal energy source. ~~Net~~Incoming shortwave radiation is not directly dependent on temperature. ~~Nor are the turbulent~~As another example, latent heat fluxes~~, which can be~~ are a significant source of energy in maritime and tropical environments (Wagnon et al., 1999, 2003; Favier et al., 2004; Anderson et al., 2010~~).~~), and their strength is a function of humidity and wind conditions, which are not strongly correlated with temperature fluctuations. This calls for a broader exploration of glacier sensitivity to climate variability and change, beyond just the influence of temperature.

~~Energy balance models have been used extensively on individual glaciers (e.g., Arnold et al., 1996; Klok and Oerlemans, 2002; Hock and Holmgren, 2005), and several~~Several studies that estimate glacier sensitivity to temperature change use complete models of ~~surface~~ energy balance (e.g., Klok and Oerlemans, 2004; Klok et al., 2005; Anslow et al., 2008; Anderson et al., 2010). ~~Assessments of glacier mass balance sensitivity have concentrated on changes~~The influence of other meteorological variables has been explored in ~~temperature and precipitation, however, and fluctuations in other variables are seldom considered.~~a few studies. Gerbaux et al. (2005) ~~explore~~examine the role of ~~other meteorological~~different variables (e.g., temperature, moisture, wind) in energy balance processes and climate sensitivity ~~of glaciers~~ in the French Alps. Giesen et al. (2008) note the importance of cloud cover in modulating interannual variability in summer melt on Midtdalsbreen, Norway. Sicart et al. (2008) examine ~~the surface energy budget on~~ three glaciers in different latitudes/climate regimes. Variations in net shortwave radiation, sensible heat flux, and temperature each contribute to differences in glacier sensitivity to climate variability between these ~~three~~ locations.

We build on these studies through a systematic examination of glacier energy balance and melt sensitivity ~~to meteorological variability at Haig Glacier in the Canadian Rocky Mountains.~~. We report the mean melt season ~~(May to September, MJJAS) and summer (JJA) meteorological and energy balance~~ conditions on ~~the~~Haig glacier in the Canadian Rocky Mountains for the period 2002-2012~~, based on an automatic weather station (AWS) in the upper ablation area (Marshall, 2014).~~. These reference data are ~~then~~ used as a baseline for theoretical and numerically modelled sensitivity ~~tests that assess the impact of changes in different meteorological parameters~~. The same perturbation approach is then used to reconstruct variations in surface energy balance and melt for the period 1979-2014, based on North American regional climate reanalyses (NARR) (Mesinger et al., 2006).

~~One of our~~ Our main ~~questions~~question is whether variables other than temperature and precipitation need to be considered to provide a realistic estimate of glacier sensitivity to climate ~~variability and~~ change for mid-latitude mountain glaciers. Our analysis ~~of summer energy and mass balance sensitivity to meteorological variability~~in this study is limited to just one site ~~in this study~~, with a focus on the summer melt season (vs. annual mass balance). We examine the summer energy balance ~~in detail, however, to~~ and evaluate the impact of different ~~weather~~ variables in isolation and with more realistic covariance of meteorological conditions~~, and to control for direct vs. indirect influences (i.e. feedbacks) on glacier melt at this site. The theoretical and energy-balance model framework for assessing glacier sensitivity that we introduce is applicable to other regions, and may help to understand regional differences in glacier sensitivity to climate variability and change.~~ .

2. Surface Energy Balance and Melt Model

The energy budget at the glacier surface is defined by the fluxes of energy between the atmosphere, the snow/ice surface, and the underlying snow or ice. The surface energy balance can be written

$$Q_N = Q_S^{\downarrow}(1-\alpha) + Q_L^{\downarrow} - Q_L^{\uparrow} + Q_H + Q_E + Q_C, \tag{2}$$

where Q_N is the net energy flux at the surface and $Q_S^{\downarrow}$, $Q_L^{\downarrow}$, $Q_L^{\uparrow}$, Q_H, Q_E, and Q_C represent incoming shortwave radiation, incoming and outgoing longwave radiation, sensible and latent heat flux, and subsurface conductive energy flux, respectively. The energy fluxes have units of W m^{-2}. The surface albedo is denoted α and fluxes are defined to be positive when they are sources of energy to the glacier surface. ~~This expression of the surface energy balance neglects~~We neglect the penetration of shortwave radiation and advection of energy by precipitation and meltwater fluxes.

The net energy Q_N can be positive or negative. When it is negative, as it is for much of the winter and during the night, the snow or ice will cool or liquid water will refreeze. Positive net energy will drive surface ~~and subsurface~~ warming, or on a melting glacier surface with $Q_N > 0$, the net energy flux is dedicated to generating surface melt~~, with~~. For melt rate $\dot{m}$, ~~following~~this follows

$$\dot{m} = \frac{Q_N}{\rho_w L_f}, \tag{3}$$

where ρ_w is the density of water and L_f is the latent heat of fusion. Melt rates in Eq. (3) have units of metres water equivalent per second (m w.e. s^{-1}).

Numerous studies have shown that incoming shortwave radiation is the dominant term in the energy balance during the melt season in most glacial environments. Incoming shortwave radiation (insolation) at the surface has three components: direct and diffuse solar radiation, along with direct solar radiation that is reflected from the surrounding terrain. Direct solar radiation is the radiative flux from the direct solar beam, which comes in at a zenith angle Z. It is a function of latitude, time of year, and time of day (e.g., Oke, 1987). Potential direct (clear-sky) incoming solar radiation on a horizontal surface can be estimated from

$$Q_\phi^{\downarrow} = Q_0 \cos(Z)\, \varphi_0^{P/P_0 \cos(Z)}, \tag{4}$$

for top-of-atmosphere insolation Q_0, clear-sky atmospheric transmissivity φ_0, air pressure P, and sea-level air pressure P_0 (Oke, 1987). Eq. (4) allows potential direct shortwave radiation to be calculated as a function of the day, year, latitude and elevation.

Longwave radiation can be estimated from the Stefan-Boltzmann equation,

$$Q_L = \varepsilon \sigma T^4, \tag{5}$$

where ε is the thermal emissivity, σ is the Stefan--Boltzmann constant, and T is the absolute temperature of the emitting surface. Snow and ice emit as near-perfect blackbodies at infrared wavelengths, with surface emissivity ε_s = 0.98-1.0. The longwave fluxes are then

$$Q_L^{\uparrow} = \varepsilon_s \sigma T_s^4, \tag{6}$$

and

$$Q_L^{\downarrow} = \varepsilon_a \sigma T_a^4, \tag{7}$$

for surface temperature T_s, near-surface air temperature T_a, and atmospheric emissivity ε_a. Terrain emissions (i.e. from the surrounding topography) can also contribute to the incoming longwave radiation, particularly at sites that are adjacent to valley walls.

A spectrally- and vertically-integrated radiative transfer calculation is needed to predict the incoming longwave radiation from the atmosphere, as this depends on lower-troposphere water vapour, cloud, and temperature profiles. Because the requisite atmospheric data are rarely available in glacial environments, $Q_L^{\downarrow}$ is commonly parameterized at a site as a function of local (2-m) temperature and humidity. Where available, cloud cover or a proxy for cloud conditions, such as the atmospheric clearness index, are often used to strengthen this parameterization. Hock (2005) and Lhomme et al. (2007) provide reviews of some of the parameterizations of atmospheric emissivity that have been employed in glaciology. We found good results for regression-based parameterization at two study sites in the Canadian Rocky Mountains (Ebrahimi and Marshall, 2015),

$$Q_L^{\downarrow} = (a + b e_v + c h)\, \sigma T_a^4 \tag{8}$$

and

$$Q_L^{\downarrow} = (a + b e_v + c \tau)\, \sigma T_a^4, \tag{9}$$

Here a, b, and c are regression parameters (different in Eqs. (8) and (9)), e_v is vapour pressure, h is relative humidity, and τ is the clearness index, calculated from the ratio of measured to potential direct incoming shortwave radiation.

Solar radiation and cloud data are less commonly available than relative humidity, so Eq. (8) is a slightly less accurate but more portable version of this parameterization (Ebrahimi and Marshall, 2015). Multiple regressions of ε_a containing both relative humidity and clearness index were rejected, as these are highly (negatively) correlated. All-sky longwave parameterizations using either of these variables are reasonable, with root-mean square errors in mean daily incoming longwave radiation of about 10 W/m^2.

Relative humidity can also be used as a proxy for clearness index if shortwave radiation data are not available. Summer (JJA) observations at Haig Glacier follow the relation:

$$\tau = 1.3 - 0.01h\,, \tag{10}$$

for mean daily values of τ and h ($R^2 = 0.5$). We draw on this below when we need to estimate perturbations in sky clearness index that are consistent with changes in atmospheric humidity. In accord with the observational basis of Eq. (10), the clearness index is constrained to be within 0.3 and 1 ($h \in [30, 100\%]$); if daily mean humidity drops below this, we set $\tau = 1$.

Turbulent fluxes of sensible and latent energy in the glacier boundary layer are ~~commonly~~ parameterized from ~~an eddy-diffusivity model of turbulent exchange~~a bulk aerodynamic method (e.g., Andreas, 2002~~), also known as the profile method:~~):

$$Q_H = \rho_a c_p k^2 v \left[\frac{T_a(z) - T_s}{\ln(z/z_0)\ln(z/z_{0H})}\right], \tag{11}$$

and

$$Q_E = \rho_a L_v k^2 v \left[\frac{q_a(z) - q_s}{\ln(z/z_0)\ln(z/z_{0E})}\right]. \tag{12}$$

Here ρ_a is the air density, c_p is the specific heat capacity of air, L_v is the latent heat of evaporation, $k = 0.4$ is von Karman's constant, v is wind speed, and q refers to the specific humidity. Measurements of temperature and humidity are assumed to be at two levels, height z (e.g., 2 m) and at the surface-air interface, s. For a melting glacier surface, $T_s = 0$°C, and q_s can be taken from the saturation specific humidity over ice at temperature T_s. We estimate T_s from an inversion of Eq. (6), using measurements of outgoing longwave radiation. In sensitivity tests, where we depart from the observational constraints, T_s is internally modelled within a subsurface snow model (see below), taken from the temperature of the upper snow layer.

Parameters z_0, z_{0H}, and z_{0E} refer to the roughness length scales for turbulent exchange of momentum, heat, and moisture. We adopt fixed values for each, equivalent for both snow and ice (z_0 = ~~1~~3 mm; $z_{0H} = z_{0E} = z_0/100$), based on closure of the surface energy balance with reference to observed melt (Marshall, 2014). Atmospheric stability adjustments can be introduced in Eqs. (11) and (12) to modify the turbulent flux parameterizations for the stable glacier boundary layer (e.g., Hock and Holmgren, 2005; Giesen et al., 2008). ~~In this study we~~ We do not apply stability corrections~~. Marshall (2014) was~~, as we are able to attain closure in modelled and measured summer melt at this site without ~~including stability corrections, and others~~this. Others have argued that stability corrections may lead to an underestimation of the turbulent fluxes on mountain glaciers (e.g. Hock and Holmgren, 2005). This may be related to the low-level wind speed maximum that is typical of the glacier boundary layer, which introduces strong turbulence and is not consistent with the logarithmic profile of wind speed that is implicit in Eqs. (11) and (12). It may also be that the effects of atmospheric stability are absorbed in the roughness values –

roughness values that are adopted to attain closure in the surface energy balance and melt calculations may be too low, implicitly accounting for the stable boundary layer.

Subsurface temperatures are modelled through a multi-layer, one-dimensional model of heat conduction and meltwater percolation and refreezing in the upper 10 m of the glacier~~. Details of the model are given in the next section. Ten meters is~~, the approximate depth of penetration of the annual temperature wave (Cuffey and Paterson, 2010). This depth includes the time-varying seasonal snow layer and the underlying firn or ice. The temperature solution follows

$$\rho_s c_s \frac{\partial T}{\partial t} = \frac{\partial}{\partial z}\left(-k_t \frac{\partial T}{\partial z}\right) + \varphi_t, \tag{13}$$

where ρ_s, c_s, and k_t are the density, heat capacity, and thermal conductivity of the subsurface snow, firn, or ice and ~~$\psi_t(z)$~~$\varphi_t(z)$ is a local source term that accounts for latent heat of refreezing,

$$\varphi_t = \rho_w L_f \dot{r} / \Delta z\,. \tag{14}$$

~~In Eq. (14), the~~The refreezing rate $\dot{r}$ has units m s^{-1}, φ_t has units W m^{-3}, and Δz is the thickness of the layer in which the meltwater refreezes.

~~We use~~Refreezing is calculated from a ~~simplistic~~hydrological model that is coupled with the subsurface thermal model. We track the volumetric liquid water fraction, θ_w, in the snow/firn pore space, and if conductive energy loss occurs in a subsurface layer where liquid water is present, this energy is diverted to latent enthalpy of freezing, rather than cooling the snow. Temperatures cannot drop below 0°C until $\theta_w = 0$. Liquid water is converted to ice in the subsurface layer.

We model meltwater drainage~~,~~ by assuming that water percolates uniformly, with hydraulic conductivity k_h and neglecting horizontal transport (i.e. assuming only gravity-driven vertical drainage). ~~For a volumetric liquid water fraction θ_w in the snow/firn pore space, local~~Local water layer thickness can be expressed $h_w = \theta_w \Delta z$. The local water balance is then

$$\frac{\partial h_w}{\partial t} = -k_h \frac{\partial h_w}{\partial z} - \dot{r}\,, \tag{15}$$

where the final term accounts for water that is ~~generated or~~ removed through internal ~~melting or~~ refreezing. In principle, this is a source/sink term that could also include internal melting (e.g., from shortwave radiation penetration or percolation of warm rainwater), but we do not consider these processes. We assume an irreducible water content of 3% for the melting snowpack (Colbeck, 1974), and the maximum volumetric water content is equal to the porosity, θ, although drainage in the seasonal snowpack is efficient and θ_w is always much less than θ.

Numerical Energy Balance and Subsurface Temperature Model

For the energy balance sensitivity experiments in this study, we use a combination of directly observed and modelled glaciometeorological variables. Where we report the directly observed surface energy balance, for the 2002-2012 reference state, we drive the energy balance model with observed 30-minute data, including measured albedo and longwave radiation fluxes. Turbulent heat fluxes and subsurface heat conduction are modelled from Equations (11-15).

Where we do sensitivity tests or run the model with other meteorological input, such as from climate models, we need to allow for internal feedbacks such as freely-determined albedo evolution and changes in incoming radiation that will attend changes in atmospheric conditions (e.g., cloud cover, humidity). The energy balance and melt model that we employ is based on daily mean meteorological inputs, in order to make our approach compatible with output from climate models or reanalyses, as well as parameterizations that operate on a daily timescale (Eqs. 8-10). A parameterized diurnal cycle is introduced for temperature and shortwave radiation (see below), in order to capture the effects of overnight refreezing and the fraction of the day that experiences melt (when Q_N and $T_s > 0$). The model ~~is run year-round with~~uses a ~~nominal~~variable time step ~~of~~from 10 minutes to 1 hour to allow for stability of the subsurface temperature prognosis.

The subsurface temperature model has 33 layers, with 10-cm layers until 0.6-m depth, 20-cm layers from 0.6-2 m, and 40-cm layers from 2-10 m. The upper boundary forcing comes from the ~~surface energy balance, which dictates either the melt rate or the temperature change in the upper surface layer. Heat~~conductive heat flux at the snow/ice-air interface, $Q_C = -k_t \partial T/\partial z$, ~~is~~ modelled from a three-point forward finite~~-~~-difference approximation of $\partial T/\partial z$. We use a two-step solution, for the temperature (Eq. 13), then the meltwater drainage (Eq. 15). The temperature solution is implicit for the temperature diffusion, with latent heat release from refreezing (the source term in Eq. 13) calculated from the previous time step~~,~~ within the hydrological model. Hydraulic conductivity in Eq. (15) is assigned the value $k_h = 10^{-4}$ m s^{-1}, near the low end of estimates reported by Campbell et al. (2006~~), and meltwater~~). Meltwater is assumed to drain instantaneously when it reaches the snow-ice interface.

The 10-m subsurface model consists of the seasonal snowpack of thickness $d_s(t)$, overlying either firn or ice. The grid is fixed with respect to the surface, and each layer is assigned a density, thermal conductivity, and heat capacity according to the medium (snow, firn, or ice). ~~Snow/firn depth is updated daily, based on daily melt totals, snowfall events, and densification through the summer melt season, May to September (see below).~~ Snow and firn density are modelled as a function of depth and the liquid water and ice content,

$$\rho_s = \rho_i(1-\theta) + \rho_w\theta_w + \rho_i\theta_i \,, \tag{16}$$

for porosity θ, liquid water fraction θ_w, and ice fraction θ_i. Densities ρ_s, ρ_i, and ρ_w refer to snow, ice and water, respectively. ~~Porosity θ decreases~~We prescribe a decrease in porosity with depth following $\theta(z) = 0.6 - 0.05z$, parameterized to~~ roughly~~ represent the measured summer snow densities at the site (ρ_s = 350-550 kg m^{-3}) and give reasonable estimates of firn density, up to ρ_s = 820 kg m^{-3} at 10-m depth.

Snow accumulates, melts, or undergoes densification on a daily time step, with snow thickness d varying continuously (vs. discretely) within the fixed-grid framework. At depth *d* below the surface, the grid cell has a weighted combination of thermal properties and densities to reflect the mixture of snow and either firn or ice in that layer. We do not have a model for snow accumulation through the winter months. We treat this simply, and linearly accumulate snow

Formatted: Left

from the start of winter until the start of the following melt season, with the accumulation rate set to give a match to the observed May snowpack thickness for each year. These data are available through annual winter mass balance surveys on the glacier, including a snowpit that provides depth and density measurements at the AWS site.

The steps in the energy balance and melt model are as follows:

1. Daily mean values are input for temperature, incoming shortwave and longwave radiation, air pressure, specific humidity, and wind speed, as well as minimum and maximum temperature.

2. A diurnal temperature cycle is parameterized as a cosine wave with a lag $\tau_t = 4$ hours to give the maximum temperature at 16:00, as per local observations, with an amplitude $A_t = (T_{max} - T_{min})/2$ (Figure 1a). For time t (hour of the day) and period $P_t = 24$ hours,

$$T(t) = -A_t \cos\left[\frac{2\pi(t-\tau_t)}{P_t}\right]. \tag{17}$$

3. A diurnal cycle for incoming shortwave radiation is parameterized as a half-cosine wave with a period $P_{sw}(d) = 2h_s(d)$, where d is the day of year and h_s is the number of hours of sunlight on day d (Figure 1b). Defining lag τ_{sw} and amplitude A_{sw},

$$Q_S^{\downarrow}(t) = \max\left\{-A_{sw} \cos\left[\frac{2\pi(t-\tau_{sw})}{P_{sw}}\right], 0\right\}. \tag{18}$$

Sunlight hours are calculated as a function of latitude, θ, and day of year, based on the equation for the sunset hour h_{ss} (e.g., Liou, 2002):

$$\cos(h_{ss}) = -\tan(\delta)\tan(\theta), \tag{19}$$

where δ is the solar declination angle (solar latitude as a function of day of year). Sunlight hours $h_s = 2h_{ss}$. The lag also varies with the day of year, and is calculated by setting peak shortwave radiation to occur at noon: $2\pi(12 - \tau_{sw})/P_{sw} = \pi$. This gives $\tau_{sw} = 12 - h_s$ hours. Amplitude A_{sw} is calculated by integrating the area under the cosine curve and equating this to the average daily incoming shortwave radiation, $Q_{Sd}^{\downarrow}$. This gives $A_{sw} = 12\pi\, Q_{Sd}^{\downarrow}/h_s$ W m^{-2}. This treatment implicitly includes cloud effects that reduce incoming shortwave radiation on a given day (via $Q_{Sd}^{\downarrow}$), but distributed evenly through the day. This neglects any systematic tendency for afternoon vs morning clouds. For simplicity, we also neglect the effect of zenith angle on atmospheric transmittance (i.e., lower transmittance for larger atmospheric path lengths in the morning and late afternoon), although this could be built into a more refined model.

4. We assume that wind, incoming longwave radiation, air pressure, and specific humidity are constant through the day, held to the mean daily value. For sensitivity tests, $Q_L^{\downarrow}$ is calculated following Eq. (8) and the daily mean value of $Q_S^{\downarrow}$ is perturbed from Eq. (10) and $dQ_S^{\downarrow} = d\tau$. ~~Relative humidity has a diurnal cycle following temperature. This impacts incoming radiation where we parameterize the sky clearness index from near-surface conditions (Eq. 10).~~

~~5.~~ 5. Relative humidity has a diurnal cycle following temperature, assuming constant daily humidity but adjusting h for consistency with the effect of temperature on saturation vapour pressure.

~~We assume that wind, incoming longwave radiation, air pressure, and specific humidity are constant through the day, held to the mean daily value. For sensitivity tests, $Q_L^{\downarrow}$ is calculated following Eq. (11) and the daily mean value of $Q_S^{\downarrow}$ is perturbed from Eq. (10) and $dQ_S^{\downarrow} = d\tau$.~~

6. Albedo is also modelled on a daily basis for the sensitivity studies. When the seasonal snowpack is melted away, albedo is set to the observed bare-ice value at the site, $\alpha_i = 0.25$. For fresh or dry snow, a fixed value $\alpha_0 = 0.86$ is used. The snowpack thickness is initialized on May 1 of each year, set to the observed value measured during the annual winter mass balance survey. During the melt season, which is assumed to start after this date, seasonal snow albedo decreases as a function of cumulative positive degree days ($\sum PDD$) following Hirose and Marshall (2013),

$$\alpha_s(d) = \alpha_0 - k_\alpha \sum PDD\,(d). \qquad (20)$$

A minimum value of 0.~~3~~4 is set for old snow ~~and firn, based on local observations. We also~~. We parameterize the effects of summer snow fall on albedo and mass balance through a ~~simple~~stochastic model of summer precipitation events~~, as described in~~ (Marshall ~~(~~, 2014). Precipitation events are set to occur randomly, with 25 events occurring from May through September as the default setting. Precipitation totals vary randomly, between 1 and 10 mm ~~in these events,~~w.e., with snow at temperatures below 0°C, rainfall above 2°C, and rain/snow partitioning increasing linearly over the range 0-2°C. Following a summer snow event, surface albedo is reset to α_0, and ~~remains at this value until melting has removed the new snow.~~its albedo begins to decay following Eq. (20). This treatment allows a natural transition to end-of-summer conditions, when fresh snowfall in September or October does not melt away.

7. Subsurface temperatures and the conductive heat flux, Q_C, are modelled with 10-minute to one-hour time steps (chosen for stability of the temperature solution~~), driven by the energy balance (Eq. 2) at the upper surface. This gives surface and internal melt totals at each time step.~~). The updated surface temperature T_s is used for the calculation of outgoing longwave radiation (Eq. 6), sensible heat flux (Eq. 11), and latent heat flux (via q_s in Eq. 12) for the next time step.

8. The hydrology model ~~is invoked to calculate~~calculates meltwater drainage and refreezing. Annual meltwater runoff is then the sum of all meltwater that drains, while summer mass balance is equal to the meltwater runoff minus the total summer snowfall, nominally for the period May 1 to September 30 at this site. This allows for some meltwater retention as either liquid water or refrozen ice within the snow or firn. We neglect water storage in the englacial and subglacial hydrology systems.

3. Field Site and Observational Data

Reference meteorological conditions, surface energy balance fluxes, and snow conditions are based on *in situ* measurements at Haig Glacier in the Canadian Rocky Mountains for the period 2002-2012 (Marshall, 2014). Winter mass balance measurements are carried out each May. These observations provide an 11-year record of observed snow depth and summer melt from an automatic weather station (AWS) located near the median elevation of the glacier, 2660 m (Figure 2). This is the upper ablation area of the glacier, which generally undergoes a transition from seasonal snow to exposed glacier ice in August.

Table 1 summarizes the mean observed meteorological and conditions at Haig Glacier over the 11-year reference period. Data coverage is incomplete, particularly in the winter months, as we transitioned to summer only measurements (May-Sept) after 2009. For the 11 years, data coverage is as follows for most sensors (e.g., temperature, shortwave radiation): JJA - 90% (909 of 1012 days); MJJAS – 86% (1441 of 1683 days); annual – 63% (2519 of 4018 days). There are more missing longwave radiation data, as the sensor was not installed until July 2003. The corresponding numbers are: JJA – 76%; MJJAS – 70%; annual – 46%.

~~The missing~~Missing data are gap-filled from a weather station that has operated continuously in the glacier forefield since 2001, at an elevation of 2325 m. The forefield AWS has more complete data coverage than the glacier AWS, above 90% for all variables. Observational data are used to adjust for the altitudinal and environmental differences between the sites, through either a monthly offset (e.g., $T_G = T_{FF} - \Delta T$), or a scaling factor β (e.g., $v_G = \beta_v v_{FF}$). Here, subscripts $_G$ and $_{FF}$ refer to the glacier and forefield AWS sites. The monthly factors are calculated from the set of all available overlapping data for the two stations. The temperature offset approach is equivalent to a lapse rate, or can be expressed that way for distributed modelling over the glacier. In this study we consider only the point energy balance at the glacier AWS site. ~~Where~~If both stations are missing data, gap-filling is done through assignment of mean daily observational data~~, in order to give 100% coverage~~.

To give a sense of the complete data record, Figure 3 shows examples of the full record, for air temperature~~ (blue line in Fig. 3a)~~, modelled surface temperature, and the ~~radiation~~energy fluxes ~~(orange~~. Average June to August (JJA) air and ~~red lines in Fig. 3b). Surface~~surface temperature are 5.2°C and ~~other surface~~ –0.6°C, respectively, and 98% of JJA days reach surface temperatures of 0°C (melting conditions) in the 11-year record. The surface energy fluxes in Fig. ~~3 are modelled. The mean annual cycles of the energy fluxes~~3b illustrate the dominance of net radiation in governing net energy at this site (Table 2).

Mean daily values for the 11-year record are plotted in Figure 4. ~~Mean daily values are plotted for the 11-year record. The four components of the shortwave and longwave radiation in Figs. 4a and 4b are combined to give the net radiation (red line in Fig. 4c).~~ As is typical for mid-latitude glaciers, ~~this~~ net radiation is the main energy flux that drives glacier melt at this site (Fig. 4c)~~.~~. Net radiation is negative in the winter, when shortwave inputs are low, albedo is high, and longwave cooling gives a radiation deficit. ~~During~~ Net radiation is positive in the summer and increases through the melt season~~, incoming~~. This is driven by increases in net shortwave radiation ~~increases and~~ as snow albedo declines ~~as snow becomes wet, particulate concentration increases, and the seasonal snow~~ at the site and then melts away to expose the underlying glacier ice (Fig. ~~4a). There is still a net longwave deficit (Fig. 4b), but outgoing longwave radiation is limited (i.e. saturates at ~315 W m^{-2}) when the surface is at the melting point. In combination, this gives surplus radiation, in~~

~~particular when low-albedo glacier ice becomes exposed~~4a). Measurements at the AWS site ~~in late July or August.~~indicate a seasonal snow albedo decrease from about 0.8 to about 0.4 each summer, which may be due to a combination of increased snow water content, grain metamorphosis in the temperate snowpack, and increasing concentration of impurities through the melt season (e.g., Cuffey and Paterson, 2010).

~~Table 2 summarizes the monthly surface energy balance fluxes at the Haig Glacier AWS site over the melt season, May through September. Mean daily melt rates are plotted in Fig. 4d, as well as the standard deviation, to give a sense of interannual variability over the period 2002-2012.~~Median daily melt rates for the period 2002-2012 are plotted in Fig. 4d, along with the interquartile range. On average, 65% of the annual glacier melt occurs in the months of July and August. Net energy peaks in August, when the low-albedo glacier ice is exposed. Sensible heat flux peaks in July, and is the other main source of energy contributing to glacier melt. On average for ~~June to August~~ ~~(~~JJA~~),~~, net radiation and sensible heat flux constitute 70% and 30% of the net energy ~~that is available for melt~~, respectively. Latent heat flux represents a small sink of energy, and conductive heat flux is a minor source of energy.

The energy balance and snowpack models have been developed and tested elsewhere (Marshall, 2014; Ebrahimi and Marshall, 2015), so we do not present the model validation in detail here. Comparisons are favorable between AWS observations (*e.g.*, in situ albedo, SR50-inferred melt), the model driven with 30-minute AWS data, and the 'daily' version of the model used here, which includes parameterizations of albedo, incoming longwave radiation, and the diurnal temperature and shortwave radiation cycles (Section 2). The simplified daily model loses some reality, but its overall performance is excellent.

As an example, glacier AWS data from summer 2015 is used as an independent test of the model, with its default parameterizations. Observed melt at the AWS site was 3.1 ±0.1 m w.e. in summer 2015, while the melt model forced by 30-minute AWS data gives 3.04 m w.e. and the parameterized, daily version of the model gives 2.98 m w.e. Taking the 30-minute AWS-driven results as the reference, the RMS error in the daily melt predictions for the parameterized model is 3% (0.7 mm w.e., relative to a daily mean value of 22.7 mm w.e.). Departures from the observations are primarily associated with the albedo, which is over-estimated in summer 2015. Overall the parameterized daily model has good skill and is an appropriate tool for the sensitivity analyses presented here.

4. Theoretical Sensitivity of the Surface Energy Balance

~~The meteorological variables in Tables 1 and 2 can be perturbed one at a time or in combination to examine the impact on modelled summer melt at the AWS site. We do this for the historical record (2002-2012) and also for the 35-year period 1979-2014, based on meteorological reconstructions from the North American Regional Reanalysis (NARR; Mesinger et al., 2006). The latter provides a more complete picture of interannual variability. Comparison of NARR predictions with measurements over the period 2002-2012 also allows us to assess the skill with~~

Formatted: Font color: Auto

Formatted: Space After: 0 pt, Line spacing: Multiple 1.08 li

~~which fluctuations in surface energy balance and summer melt can be captured in an atmospheric model that does not explicitly resolve the alpine and glacier conditions.~~

Surface energy balance processes and summer melt rates depend on various meteorological influences ~~in~~ (Eqs. ~~(~~4-11). Warm summers generally cause high melt rates and promote negative mass balance, but the energy balance is sensitive to other weather conditions as well. ~~We~~To examine these sensitivities ~~for atmospheric conditions that are typical of~~, meteorological variables in Tables 1 and 2 can be perturbed one at a time or in combination to examine the impact on summer melt ~~season on mid-latitude glaciers. For quantitative illustration, we adopt~~at the ~~average June to August (~~Haig Glacier AWS site. Perturbations are introduced with respect to the mean JJA~~)~~ meteorological conditions from 2002-2012 ~~at Haig Glacier in the Canadian Rocky Mountains (Tables 1 and 2):~~ ~~$T_a = 5.1°C$, $h = 67\%$, $e_v = 5.7$ hPa, $q_v = 4.8$ g/kg, $P = 750$ hPa, $v = 2.6$ m/s, $Q_S{\downarrow} = 226$ W/m^2, $Q_\phi{\downarrow} = 359$ W/m^2, $\tau = 0.63$, $\alpha = 0.55$, and $Q_L{\downarrow} = 280$ W/m^2. Mean weather conditions and surface energy balance conditions in Tables 1 and 2 are typical of mid-latitude mountain glaciers~~.

~~Average JJA melt at~~ Theoretical sensitivities are calculated in this section by differentiating the ~~Haig Glacier AWS site was 2320 mm w.e.~~net energy balance with respect to each meteorological variable. This is akin to generating a Jacobian matrix for Q_N, based on partial derivatives of the dependent variables in the surface energy balance. One cannot gauge the most important meteorological influence on surface energy and mass balance from ~~2002-2012.~~ the sensitivities to a unit change in each variable. For instance, a change in specific humidity of 1 g kg^{-1} equals 3.3 standard deviations, with respect to the interannual (JJA) variability (Table 1). In contrast, summer temperature has a standard deviation of 0.8°C, so a 1°C temperature change is a smaller perturbation. To allow a direct comparison of the theoretical sensitivities and to give a simple representation of their natural, interannual variability, we perturb each variable by one standard deviation, based on the values reported in Tables 1 and 2.

We consider the ~~main~~core summer months ~~here~~, JJA, to calculate the theoretical sensitivity because ~~more~~the glacier surface is at melting point for most of this time (Fig. 3a), which is a necessary condition to relate net energy to melt. More than 80% of the annual melt also occurs in this season~~,~~ (Table 2 and Fig. 4d), so meteorological forcing over this period has the highest impact on glacier melt. ~~Weather conditions also matter in the shoulder months, May and September, but anomalies in these months have less impact on glacier melt and mass balance. We repeat the sensitivity analysis for MJJAS conditions, and present a summary of these results. Melt model experiments in the next section consider the energy balance from May through September, in order to capture the complete melt season.~~

Sensitivity to Temperature

Air temperature appears directly in the expressions for $Q_L{\downarrow}$ and Q_H. Temperature change may also influence the surface energy balance through influences on other variables, such as atmospheric moisture (Q_E). For a melting glacier surface, where surface and subsurface temperatures are at 0°C, air temperature changes do not directly influence $Q_L{\uparrow}$ or Q_C. To estimate the magnitude of temperature sensitivity, we differentiate each energy balance flux with respect to temperature.

Formatted: Normal

Formatted: Normal

Formatted: Normal

For incoming longwave radiation, Eq. (7), the resulting temperature sensitivity is:

$$\frac{\partial Q_L^{\downarrow}}{\partial T} = 4\sigma\varepsilon_a T_a^3 + \sigma T_a^4 \frac{\partial \varepsilon_a}{\partial T}. \tag{21}$$

This general form applies to a range of formulations for ε_a, such as those of Brutsaert (1975), Lhomme et al. (2007), or Sedlar and Hock (2009). Adopting the parameterization in Eq. (8), which performs well at Haig Glacier,

$$\frac{\partial Q_L^{\downarrow}}{\partial T} = 4\sigma\varepsilon_a T_a^3 + \sigma T_a^4 \left(b\frac{\partial e_v}{\partial T} + c\frac{\partial h}{\partial T}\right). \tag{22}$$

The last two terms reflect potential feedbacks of temperature change on humidity. While we are only considering perturbations to temperature in this section, vapour pressure and relative humidity cannot both remain constant under a temperature change. We first assume that relative humidity h remains constant, under which conditions we assume that cloud cover and sky clearness will be unchanged. For constant h, e_v scales with temperature following the Clausius-Clapeyon relation for saturation vapour pressure,

$$\frac{\partial e_v}{\partial T} = \frac{h}{100}\frac{\partial e_s}{\partial T} = \frac{h}{100}\left(\frac{L_v e_s}{R_v T_a^2}\right) = \frac{L_v e_v}{R_v T_a^2}, \tag{23}$$

where $R_v = 461.5$ J kg^{-1} °C^{-1} is the gas law constant for water vapour.

For the mean JJA meteorological conditions at Haig Glacier, Eqs. (22) and (23) give $\partial Q_L^{\downarrow}/\partial T =$ 4.7 W m^{-2} °C^{-1}. Temperature increases affect $Q_L^{\downarrow}$ through both the direct effect of higher emission temperatures and the indirect effect of higher atmospheric emissivity, with these two terms in Eq. (21) contributing 4.0 and 0.7 W m^{-2} °C^{-1}, respectively.

The temperature sensitivity of sensible and latent heat fluxes follow

$$\frac{\partial Q_H}{\partial T} = \frac{\rho_a c_p k^2 v}{\ln(^z/_{z_0})\ln(^z/_{z_{0H}})}, \tag{24}$$

and

$$\frac{\partial Q_E}{\partial T} = \frac{\rho_a L_p k^2 v}{\ln(^z/_{z_0})\ln(^z/_{z_{0E}})}\left(\frac{\partial q_v}{\partial T}\right), \tag{25}$$

where

$$\frac{\partial q_v}{\partial T} \approx \frac{R_d}{P R_v}\left(\frac{\partial e_v}{\partial T}\right), \tag{26}$$

for the dry gas-law constant $R_d = 289$ J kg^{-1} °C^{-1} and air pressure P, under the assumption that air pressure and density are constant for small changes in temperature. Table 3 gives the turbulent flux sensitivities for mean JJA conditions at Haig Glacier. Perturbations to both Q_H and Q_E are positive with an increase in temperature and the assumption of constant h. In combination with the increase in $Q_L{}^{\downarrow}$, net energy over the summer months is augmented by 12 W m^{-2} for a 1°C increase in temperature. Interannual variations in summer temperature (1σ) equal 0.8°C, giving a net energy perturbation $\delta Q_{N\sigma}$ = +10 W m^{-2} (Table 3).

~~Energy~~Fluctuations in energy balance ~~perturbations~~ can be related to melt rates through their combined influence on Q_N, with $\delta\dot{m} = \delta Q_N / \rho_w L_f$. -Table 3 summarizes these impacts on summer melt, assuming a JJA melt season (92 days). The 1~~°C~~-σ temperature increase (δQ_N ~~= 12~~$_\sigma$ = 10 W m^{-2}) is equivalent to ~~295~~236 mm of meltwater at the AWS site, ~~if melting conditions prevail and this energy can all be directed to snow/ice melt. This is a 13~~a 10% increase over the reference ~~levels of~~ JJA melt, 2320 mm w.e. These are the direct impacts of higher temperatures, not accounting for feedbacks or non-linearity in the seasonal evolution of melt conditions. -These calculations assume that melting conditions prevail throughout the summer and all of this energy can be directed to snow/ice melt, which is not strictly true. We include them because estimates of the potential influence on summer melt provide an intuitive way to understand and compare sensitivities. We consider more realistic relations between net energy and melt in the modelled sensitivities of Section 5.

This initial scenario assumes that the warmer atmosphere contains more moisture, which is not necessarily the case. For instance, high summer temperatures in this region are commonly associated with ridging and subsidence, i.e. hot, dry conditions. If we assume that ~~e_v~~q_v is invariant with temperature (case 2 in Table 3), there is no feedback on the latent heat flux and the increase in net energy is less than with constant h: δQ_N ~~= 8.3~~$_\sigma$ = 6.6 W m^{-2} and δm ~~= 196~~$_\sigma$ = 157 mm w.e.

However, ~~this neglects~~there are additional feedbacks associated with relative humidity. If ~~e_v~~q_v is invariant, relative humidity must change to be consistent with the temperature perturbation. ~~An~~As an example, an increase of 1°C with no change in ~~e_v~~q_v corresponds to a decrease of 6% in mean summer h at our site, to 61%. This lowers the atmospheric emissivity in Eq. (8), reduces the incoming longwave radiation, and impacts $\partial\varepsilon_a/\partial T$ in Eq. (22). To be internally consistent, reduced humidity ~~will~~anomalies should also be associated with ~~decreased~~changes in cloud cover. For the 1°C temperature increase, the 6% decrease in relative humidity corresponds to an increase in clearness index of 0.06 (Eq. 10), from 0.63 to 0.69.

The effects of these radiation feedbacks are given in Table 3. Reduced relative humidity decreases $Q_L{}^{\downarrow}$ and increases $Q_S{}^{\downarrow}$. The resulting increase in shortwave radiation partially offsets the decline in $Q_L{}^{\downarrow}$, but there is an overall reduction in net radiation. For our parameterizations of the incoming radiation fluxes as a function of humidity, the effect of drier air on longwave radiation is stronger than the shortwave radiation feedback. This reduces the overall sensitivity to temperature change relative to the first two cases, with δQ_N ~~= 6.6~~$_\sigma$ = 5.3 W m^{-2} and δm ~~= 156~~$_\sigma$ = 125 mm w.e. Note that ~~all of~~ these temperature scenarios are all idealized, neglecting albedo feedbacks and other indirect effects of a temperature change. These feedbacks are ~~discussed and~~ assessed in Section 5.

Sensitivity to Humidity and Wind

Similar derivatives and energy balance sensitivities can be derived with respect to the other meteorological variables, to explore the sensitivity of summer melt to different weather conditions. The sensitivity of sensible and latent heat fluxes to wind perturbations follow:

Formatted: Justified

Formatted: Font: 4 pt

$$\frac{\partial Q_H}{\partial v} = \frac{\rho_a c_p k^2 (T_a - T_s)}{\ln(z/z_0)\ln(z/z_{0H})} \ , \tag{27}$$

and

$$\frac{\partial Q_E}{\partial v} = \frac{\rho_a L_p k^2 (q_v - q_s)}{\ln(z/z_0)\ln(z/z_{0E})} \ , \tag{28}$$

while the sensitivity to humidity is:

$$\frac{\partial Q_E}{\partial q_v} = \frac{\rho_a L_p k^2 v}{\ln(z/z_0)\ln(z/z_{0E})} \ . \tag{29}$$

Incoming longwave radiation is also affected by perturbations in humidity, following:

$$\frac{\partial Q_L^{\downarrow}}{\partial q_v} = \sigma T_a^4 \frac{\partial \varepsilon_a}{\partial q_v} = \sigma T_a^4 \left(b \frac{\partial e_v}{\partial q_v} + c \frac{\partial h}{\partial q_v} \right) . \tag{30}$$

Table 3 summaries the theoretical sensitivities for specific humidity and wind perturbations of 1 g kg^{-1} and 1 m s^{-1}, respectively, assuming that temperature is unchanged. For the humidity, we present two scenarios: the first with perturbations to only the specific and relative humidity, and the second including the expected effects of an increase in relative humidity on cloud cover.

Changes in humidity directly impact the latent heat flux, and may also influence incoming longwave radiation and cloud cover (hence, incoming shortwave radiation). We consider the effects of a humidity perturbation with and without radiative feedbacks in Table 3. For $\delta q_v = 1$ g kg^{-1} and fixed temperature, mean summer relative humidity increases by 12%, to 79~~%.~~%, and Q_E ~~increases~~ and Q_N increase by 10.5 W m^{-2}. Interannual variations in q_v equal 0.3 g kg^{-1}, giving $\delta Q_{N\sigma}$ = 3.2 W m^{-2}, corresponding to a ~~250~~76-mm (~~11~~3%) increase in summer melt.

Where radiation feedbacks are included, the increases in specific and relative humidity have a strong influence on the atmospheric emissivity in Eq. (8), giving an increase in $Q_L^{\downarrow}$ of 24 W m^{-2}. This is partially offset by cloud feedbacks associated with the increased humidity. Following Eq. (10), δh = 12% equates to a decrease in atmospheric transmissivity of 0.11, which strongly attenuates incoming shortwave radiation. This reduces the ~~radiative and~~ net ~~energy~~radiation by 19 W m^{-2}, but the radiation feedbacks remain positive. The net impact of a 1-σ humidity perturbation δq_v = ~~1~~0.3 g kg^{-1} is then ~~16~~4.7 W m^{-2}, corresponding to a ~~370~~112-mm (~~16~~5%) increase in summer melt.

Wind perturbations have straightforward linear effects on Q_H and Q_E, ~~with~~giving a ~~theoretical~~net sensitivity ~~of~~ $\partial Q_N/\partial v$ = +7 W m^{-2} ~~for an increase in summer winds of 1~~ (m s^{-1})$^{-1}$. Sensible heat flux increases and evaporative cooling decreases slightly. Winds have a low interannual variability at this site, 0.2 m s^{-1}, so the associated net energy anomaly is $\delta Q_{N\sigma}$ = 2 W m^{-2}, equivalent to 50 mm w.e. in summer melt.

Formatted: Font: Not Italic

Formatted: Font: 6 pt

~~Changes in Net Shortwave~~ Sensitivity to the Radiation Fluxes

Net shortwave radiation is ~~not directly dependent on air temperature, but is~~ affected by variations in ~~incoming shortwave radiation~~top-of-atmosphere insolation, the clearness index (i.e. cloud conditions), and surface albedo. ~~Incoming shortwave radiation changes due to solar variability, e.g., sunspot cycles, or through variations in the atmospheric transmissivity or clearness index, though, e.g., the effects of aerosols and cloud cover.~~ Our functional relationship for net shortwave radiation is $Q_{Snet} = Q_S^{\downarrow}(1-\alpha_S) = Q_{S\phi}\tau(1-\alpha_S)$, for potential direct insolation $Q_{S\phi}$ and clearness index τ. From Eq. (4), sensitivity to top-of-atmosphere insolation Q_0 follows

$$\frac{\partial Q_{Snet}}{\partial Q_0} = \tau\,(1-\alpha_S)\cos(Z)\,\varphi_0^{P/P_0\cos(Z)}\,, \tag{31}$$

~~Sensitivity to the clearness index follows~~

$$\cancel{\frac{\partial Q_{Snet}}{\partial \tau} = Q_{S\phi}(1-\alpha_S)\,,} \tag{32}$$

~~and the albedo sensitivity is~~

$$\cancel{\frac{\partial Q_{Snet}}{\partial \alpha_S} = -Q_{S\phi}\tau\,.} \tag{33}$$

~~The insolation perturbation shown in Table 3, $\delta Q_S^{\downarrow} = 0.6$ W m^{-2}, corresponds to a 1 W m^{-2}~~ An anomaly of 1 W m^{-2} in the top-of-atmosphere insolation, Q_0, ~~in Eq. (31). This is reduced to 0.6 W m^{-2} as a result of the mean sky clearness index of 0.63,~~ gives $\delta Q_S^{\downarrow} = 0.6$ W m^{-2}, and the net radiation impact is further reduced to 0.3 W m^{-2} by the surface albedo.

~~This is consistent with a direct estimate of sensitivity to variations in solar output through Eq. (31). For summer solstice at Haig Glacier (50.7°N, 2660 m altitude) and for $\varphi_0 = 0.84$ (clear-sky conditions), $\partial Q_{Snet}/\partial Q_{S0}$ in Eq. (31) can be integrated over the daily solar path. For a 1 W m^{-2} change in top-of-atmosphere radiation, Q_0, this gives a daily mean net shortwave perturbation of 0.25 W m^{-2} at the surface. Even with clear-sky conditions, only 25% of the solar perturbation is felt at the glacier surface. The~~ The net impact of ~~daily and interannual~~ top- of-atmosphere solar variability ~~(e.g.,~~, such as sunspot cycles~~)~~, is therefore small.

~~Incoming shortwave~~In contrast, incoming radiation fluxes and energy balance are ~~more~~strongly sensitive to ~~cloud cover, as captured through the sky clearness index, τ, although this is also muted by the surface albedo. An increase in τ of 0.05, from 0.63 to 0.68, translates to an increase in net energy of 8 W m^{-2} and a 5% increase in summer melt. Note that it could also be possible to work with~~ atmospheric transmissivity, ~~φ, in Eq. (32), rather than the clearness index, but our parameterizations of~~ which in turn is largely governed by cloud cover. Direct, independent variations in incoming shortwave and longwave radiation are reported in Table 3 for fluctuations of 10 W m^{-2} and for 1-σ variations in each. Sensitivity is moderate, of order 6% of the net energy.

It is more appropriate to consider co-variations of these radiation fluxes that can be expected in association with changes in cloud cover ~~and~~. We can estimate through the sky clearness index, τ, as parameterized via Eqs. (9) and (10), which relate the atmospheric ~~transmissivity are through τ~~

~~(Eqs. 9 and 10), so we use this framework here.~~emissivity and relative humidity to clearness index. As an example, reduced cloud cover may be associated with a 1-σ increase in τ of 0.1, from 0.63 to 0.73. This translates to an increase in net shortwave energy of 16 W m^{-2} (Table 3), but the change in cloud cover also impacts incoming longwave radiation. Clearer skies in the example of Table 3 give lower h, lower e_v, and lower $Q_L^{\downarrow}$. Latent heat flux also declines. The overall result is a reduction in net energy for an increase in τ. A 1-σ increase (+0.04) gives a 3% reduction in net energy.

Sensitivity to Albedo

The sensitivity to albedo changes is comparatively high. An ~~increase~~change in albedo of 0.1 creates ~~a peak~~an energy balance perturbation of more than 100 W m^{-2} at local noon in mid-summer. The magnitude of this effect varies with latitude, time of year, and atmospheric transmissivity. Integrated over the daily solar path and over the summer, an albedo increase of 0.1 reduces net solar radiation by –23 W m^{-2}~~, giving a 24% decrease in total summer melt~~. Measurements at the site indicate an interannual albedo variability of 0.06, equivalent to 14% of the net energy or $\delta m_{\sigma} = -323$ mm w.e.

~~One cannot gauge the most important meteorological variable to surface energy and mass balance from the sensitivities to a unit change in Table 3, as some meteorological parameters are intrinsically more variable. For instance, the sensitivity to a change in humidity appears to be comparable to the sensitivity to temperature, but an increase in humidity of 1 g kg^{-1} equals 3.3 standard deviations, with respect to the interannual (JJA) variability (Table 1). In contrast, summer temperature has a standard deviation of 0.8°C, so the 1°C temperature increase in Table 3 is a weaker perturbation. Similarly, a sustained wind anomaly of 1 m s^{-1} is a large perturbation, relative to a standard deviation of 0.2 m s^{-1} in mean summer winds recorded at the site from 2002-2012.~~

~~To allow a direct comparison, we perturb each variable by one standard deviation (cf. Table 1) in the direction of increased melt: higher temperature, humidity, wind speed, incoming shortwave radiation, and a lower albedo. This might be representative of warm, sunny summer weather that causes high melt extent, but within the observed range of variability at Haig Glacier. The experiment assumes that weather conditions all align in a way to increase the net energy, which will not be true in general (e.g., warm summers are typically dry in the region).~~

~~Results are given in the last two lines of Table 3, for both mean JJA and mean MJJAS conditions. For the main summer months, JJA, Q_N is augmented by 34.6 W m^{-2}, giving a 35% (821 mm) increase in summer melt. Increases in each component of the surface energy balance contribute to this, but shortwave radiation is the strongest component, accounting for about half of the elevated melt. This is due to both an increased clearness index (i.e. clear-sky conditions) and the decreased albedo. None of the surface energy fluxes is negligible in the perturbed energy budget. The turbulent flux increases are mostly due to the increases in temperature and humidity. Over a summer melt season, energy balance and melt anomalies are relatively insensitive to variations in wind speed. This is not true on short timescales, where windy periods strongly affect the turbulent heat fluxes.~~

~~Results are similar for the 1-σ perturbation in MJJAS conditions, with an increase in Q_N of 33.5 W m^{-2}. The net shortwave radiation again accounts for about half of this perturbation. If this energy balance anomaly is maintained over a five-month period (and assuming melt conditions for this whole period), it equates to an additional 1320 mm of melt, a 43% increase over the mean value for the period 2002-2012.~~

Summary

Overall, the results indicate a strong sensitivity of the summer energy balance and melt to temperature and albedo, with weaker influences from cloud conditions, humidity, and wind speed. These theoretical sensitivities are ~~obviously~~ idealized, however, and neglect ~~some~~many important feedbacks and glaciometeorological interactions that occur in glacier environments. The next two sections ~~examines~~examine the energy balance sensitivity at Haig Glacier within an energy balance-melt model. This allows an estimate of feedbacks associated with the evolution of albedo, interannual variability in weather conditions, and meteorologically-consistent covariance of weather variables.

5. Modelled Sensitivity of the Surface Energy Balance

We use a point model of surface energy balance, described in detail in Section 2. ~~Depending on the sensitivity study (i.e. controlling for different variables or letting them freely evolve),~~For all numerical experiments described below, we use ~~either: (i) the direct measurements of radiation fluxes and surface albedo, or (ii)~~the daily model with parameterizations of the longwave radiation fluxes, atmospheric clearness, diurnal cycles of temperature and shortwave radiation, and surface albedo evolution, following Eqs. (6), (8), (10), (17), (18), and (20). Surface temperature is modelled from the subsurface temperature model. The mean daily forcing for the energy balance and snowpack models is taken from the glacier AWS data, and the model is run year-round for the period 2002-2012. The May 1 snowpack thickness (winter accumulation) is specified for each year based on the measured winter mass balance at the AWS site.

Perturbations to the observed weather~~ from 2002-2012~~ are used to repeat the sensitivity analyses of section 4, but with a realistic evolution of each summer melt season rather than the mean summer conditions. Meteorological variables are perturbed as follows: ±2°C for temperature, ±50% for specific humidity and wind, ±~~20 W m^{2} for incoming shortwave radiation,~~0.1 for the sky clearness index (a proxy for cloud cover), and ±0.1 for albedo. Increments are set to give 41 realizations in each case, spanning the range of the perturbation. For example, temperature increments of 0.1°C are applied for the range –2 to 2°C. Each perturbation is prescribed for all days in the original data, and the energy balance program is run for the period 2002-2012. In each experiment, all other meteorological variables are held constant except for those that are direct impacted by a perturbation (e.g., relative humidity changes with temperature).

Table 4 lists the response of mean summer (JJA) net energy, Q_N, to the different meteorological perturbations. Changes in the energy fluxes can be examined in response to the perturbations, e.g., ΔQ_N as a function of temperature anomalies, δT. We plot these values to give sensitivity curves (e.g., Figures 5 and 6), and the slope of each curve is a measure of the sensitivity, e.g., dQ_N/dT.

Values in Table 4 are calculated through linear regression. The relationships area generally nonlinear, so we compute the regressions for the region of the sensitivity curve within ±1 standard deviation (±1 σ) of the reference value for each variable. This samples a more linear range and allows a better comparison with the derivatives in Table 3. Standard deviations refer to the interannual variability, as reported in Table 1. Table 4 also lists the change in net energy associated with a 1-σ increase in each variable.

There are multiple scenarios for temperature, shown in the first four cases in Table 4. These cases represent different assumptions about the way in which atmospheric moisture and radiation fluxes respond to a temperature perturbation. The first two cases follow the assumption that relative humidity does not change. Hence, a temperature change δT is attended by a change in specific humidity, δq_v, to maintain constant h. This impacts latent heat flux and atmospheric emissivity. Cases 1 and 2 show the net energy sensitivity to this scenario without and with albedo feedbacks. The next two cases include albedo feedbacks, but assume no change in specific humidity, $\delta q_v = 0$; hence relative humidity must respond. Cases 3 and 4 are without and with atmospheric radiation feedbacks to the changed relative humidity.

Summer melt sensitivity for the four different temperature perturbation scenarios is plotted in Figure 5. Case 1~~, the purple line in Fig. 5,~~ lacks albedo feedbacks and ~~indicates~~ corresponds to a net energy sensitivity of ~~10~~13 W m^{-2} C^{-1}, which is comparable to the theoretical temperature sensitivities in Table 3. This is ~~through~~due to direct temperature/humidity impacts on incoming ~~longwave~~ radiation fluxes, sensible heat flux, and latent heat flux. Cases 2-4 include albedo feedbacks. This can be considered to be more realistic, and the albedo feedbacks have a ~~powerful~~ ~~(~~roughly ~~5~~two-fold~~)~~ amplification effect on the temperature perturbation. Under constant h, dQ_N/dT = ~~55~~27 W m^{-2} C^{-1} (~~black line in Figures 5 and~~cf. Figure 6a), representing a ~~57~~28% increase in summer melt for a 1°C warming. This decreases by ~~4–12~~6-10 W m^{-2} C^{-1} in cases 3 and 4, where q_v is held constant. Some of the reduced energy comes from the elimination of latent energy feedbacks. Case 4, with atmospheric radiation feedbacks, reduces energy further as ~~increased~~decreased cloud cover (via higher τ) reduces incoming ~~shortwave~~longwave radiation more strongly than it ~~increase longwave~~ increases shortwave fluxes in the model. Here too, the numerical model gives a similar result to the theoretical prediction.

Figure 6a plots the response of the different surface energy fluxes for ~~case 2 above. Here it can be seen that net radiation (via the absorbed~~the reference model, case 2. Net shortwave radiation~~)~~ dominates the temperature response, over Q_H, Q_E, and $Q_L{\downarrow}$. ~~The relationship is nonlinear, with a weaker response at higher and lower temperature perturbations. This is likely associated with weaker albedo feedbacks when the snowpack is either persistent through the full summer (large negative δT) or is removed quickly in the early summer (large positive δT).~~

Figures 6b-6d provide similar details for perturbations in humidity, wind, ~~shortwave radiation~~clearness index, and albedo (cases 5-9 in Table 4). Sensitivity to humidity changes is relatively strong, through the combined impacts of latent and longwave fluxes (Fig. 6b). Case 6 is shown in this figure, including feedbacks on the atmospheric radiation. Incoming longwave radiation~~ (orange line in Fig. 6b)~~ is strongly augmented by the increases in absolute and relative humidity, and accounts for about 70% of the net energy sensitivity to specific humidity. It is partially offset by cloud feedbacks, however, ~~such that the net radiation (red line) sensitivity is~~

~~much less, and is comparable to the latent heat flux sensitivity.~~which reduce incoming shortwave radiation.

For increases in both temperature and humidity, the mean summer latent heat flux switches sign from negative (Table 2) to positive; that is, latent heat flux becomes a source rather than sink of energy under warmer and wetter conditions. In contrast, latent heat flux remains negative, but small, under increases in wind speed (Figure 6c). Energy balance sensitivity to wind perturbations is primarily associated with the sensible heat flux.

~~Shortwave radiation~~ Net energy perturbations due to albedo and clearness index in Figure 6d are independent of each other, but are plotted together for convenience. ~~Net energy sensitivity to perturbations in incoming shortwave radiation are attenuated through the albedo, which reduces the impact of changes in top-of-atmosphere insolation or atmospheric transmissivity on surface energy variability.~~ Albedo sensitivity over ~~a~~the range ~~of~~ ±0.1 is relatively high, with a decrease in net energy of ~~22~~27 W m^{-2} (~~23~~28%) for an increase in albedo of 0.1.

~~The sensitivities computed with the surface energy balance model are generally consistent with the theoretical sensitivities in Section 4, with the exception of the strong amplification introduced by albedo feedbacks. For realistic perturbations, such as a 1-σ increase in each variable, sensitivity to temperature is far higher than for the other variables. Interannual variations in albedo are the next strongest influence, followed by incoming shortwave radiation (i.e.~~ Changes in sky clearness index (atmospheric transmissivity) have a lower impact, due to the compensating influences on incoming shortwave and longwave radiation. Reduced cloud cover~~) and humidity. Interannual variations in wind have only a minor influence on the summer energy budget.~~ (higher τ) gives an overall reduction in net energy at our site, as longwave radiation effects are dominant.

Formatted: Left

Sensitivity to Winter Snow Accumulation

Changes in the winter mass balance ~~– the spring snowpack – have an additional~~also influence ~~on the evolution of~~ the summer melt season~~, which we have not examined above.~~. Interannual variability in the ~~snowpack~~amount of snow is implicit in the simulations, as the spring (May 1) snowpack depth is initialized with the measured winter mass balance~~, b_w, as measured at the AWS site~~ – for each ~~May~~year, b_w (Marshall, 2014). However, ~~we have~~these experiments do not ~~controlled~~control for ~~this~~the influence of snow depth on summer melt extent.

To examine this, we ~~use the mean annual meteorological record from 2002-2012 and use this to~~ force the energy balance model ~~through~~over a range of winter mass balance conditions, $b_w \in [0.36, 2.36]$ m w.e. ~~The~~This is ±1 m w.e. relative to the mean observed value ~~from 2002-2013 was~~at the AWS site, 1.36 ± 0.27 m w.e. ~~at the AWS site.~~The melt model is run through 11 years of weather, 2002-2012, with the different values of winter mass balance as an initial condition. Figure 7 plots the ~~modelled~~average evolution of ~~the~~ seasonal snowpack depth and albedo ~~through the summer melt season,~~ from May through September~~,~~ for this suite of experiments. ~~The snowpack depth is expressed in meters, as used for the subsurface temperature model. Fig. 7c shows the~~ Transitions from seasonal snow to ice span from early July to mid-September. Albedo spikes in Fig. 7b are due to summer snow events, which become more frequent as temperatures cool in September.

The net energy balance ~~perturbation~~perturbations that ~~accompanies~~accompany these scenarios~~.~~ ~~There is relatively little effect at this site~~ are shown for ~~the deeper snowpacks, once the seasonal snow is thick~~two choices of the minimum snow albedo (Fig. 7c). Observations of late-summer snow at the site are in the range 0.3-0.4, the two values presented here. The plot is asymmetric; net energy is more sensitive to reduced winter snow depths, which result in an earlier transition to exposed glacier ice. A 20% (1 σ) reduction in b_w gives a net energy increase of about 4 W m^{-2} (4%), and the sensitivity increases non-linearly with increasingly lower snow depths. The influence from a deep winter snowpack is comparatively muted: 1-2 W m^{-2} reductions in Q_N for a 20% increase in the winter snow thickness. Perturbations in Q_N asymptote once seasonal snow is deep enough to survive through the summer. ~~For low values of b_w, net energy increases by about 10 W m^{-2} (10%). This is~~

The influence of the winter snowpack at this site is similar in magnitude to the net energy impacts of interannual variations in ~~the humidity or~~ wind speed, but less important to the summer melt than observed variations in ~~summer~~ temperature, albedo, or cloud cover. This result is partly due to the relatively low contrast between late-summer snow albedo and bare-ice albedo at this site. If late-summer snow has a higher albedo, a deep winter snowpack is more effective at reducing the net energy and summer melt. The shape of the sensitivity curve would change for locations with higher-albedo snow, and also for sites in the lower ablation zone, where ice is exposed early in the melt season. A heavy winter snowpack would have a comparatively stronger role in this case. The result in Figure 7 is therefore more site-specific than for the other meteorological perturbations.

Formatted: Justified

6. NARR-based Surface Energy Balance Reconstructions, 1979-2014

To examine energy balance sensitivity over a longer time period and with joint variation in meteorological variables, we run the energy balance model forced by North American Regional Reanalysis (NARR) atmospheric reconstructions from 1979 to 2014 (Mesinger et al., 2006). This provides a more complete picture of interannual variability, while comparison of NARR predictions with measurements over the period 2002-2012 also allows us to assess the skill with which fluctuations in surface energy balance and summer melt can be captured in an atmospheric model that does not explicitly resolve the alpine and glacier conditions.

We use a perturbation approach as in Section 5, taking NARR daily meteorological fields as anomalies relative to the mean NARR conditions for the period 2002-2012. Anomalies in near-surface temperature, specific humidity, wind speed, pressure, incoming shortwave radiation and incoming longwave radiation are used to drive the model for the 36-year period 1979-2014. ~~*in situ* conditions for the period 2002-2012. The main difference from Section 5 is that~~Perturbations are introduced as anomalies relative to the mean observed conditions. NARR input fields allow us to introduce multiple perturbations at once, with magnitudes that are physically meaningful and meteorologically-consistent covariance of variables.

NARR has an effective spatial resolution of 32 km, and we extract mean daily data from the grid cell over Haig Glacier. This grid cell has an elevation of 2214 m, about 450 m lower than the AWS site. ~~Anomalies in near-surface temperature, specific humidity, wind speed, pressure, incoming shortwave radiation and incoming longwave radiation are used to drive the model for the 36-year period 1979-2014.~~ By using daily weather anomalies, we avoid most biases associated with the different altitude of the NARR grid cell. However, variations in some fields such as specific humidity, pressure, and temperature can be larger at lower elevations and over non-glacierized land surface types. Since we use meteorological fluctuations as perturbations, this is potentially problematic. Inspection of the summer variance in the different meteorological inputs over the ~~36-year~~reference period 2002-2012 indicates that this does not appear to be an issue~~, however~~. Standard deviations of each variable, calculated from mean JJA values, are as follows: temperature, 0.8°C; specific humidity, 0.~~3~~2 g kg^{-1}; wind speed, 0.~~2~~3 m s^{-1}; incoming shortwave radiation, ~~7~~6 W m^{-2}; and incoming longwave radiation, ~~4~~3 W m^{-2}. Temperature, humidity, and wind values are ~~identical~~equivalent to the observed range of variability from 2002-2012 (Table 1), but the radiation fluxes are less variable. The effects of a lower elevation in the NARR grid cell appear to be less than those associated with systematic biases in the reanalysis, e.g., not enough variability in cloud ~~or surface~~ conditions.

The energy balance model requires an estimate of winter snow accumulation. We base this on cumulative NARR precipitation for the period September to May of each year, normalized to the observed value of 1.36 m w.e. at the Haig Glacier AWS site. This permits interannual variability in the winter snowpack thickness to be included in the simulations, by scaling the mean observed value up or down based on the NARR winter precipitation totals. We use this as an initial condition for the ~~summer~~ melt model~~. Our focus is on the summer energy budget and~~ (i.e., for May 1 snow~~/ice melt, rather than annual mass balance reconstructions.~~ depth).

We examine the sensitivity of net summer energy balance and melt to interannual variations in each weather variable in the NARR forcing. Table 5 reports the NARR-based surface energy fluxes and melt for JJA and MJJAS, averaged over the period 1979-2014. Mean values are all within 2 W m^{-2} of the reference surface energy fluxes (Table 2), derived from the in situ data, but there are some significant differences in the standard deviation, which is a measure of the interannual variability. As noted above, incoming shortwave radiation has about half of the variability in the 36-year NARR record as observed in the 11-year measurement period, and variance in incoming longwave radiation is also less than observed. This implies more uniform summer cloud conditions in the reanalysis, compared to the observational period.

Average summer albedo is also less variable in the model than the observations~~. The~~, and the mean value in the NARR-forced model is ~~also lower than the observations, particularly~~too low for May through September (0.55 vs. an observed value of 0.60). Most of this difference is associated with a low value of September albedo in the model; we are ~~likely~~generally underestimating September snow events and predicting too late a transition from end-of-summer to the winter accumulation season. This transition occurs sometime in September or October each year in our study period. September is mixed on the glacier, with fresh snowfall alternating with periods of melting. This raises the average albedo on the glacier, but our albedo parameterization does not fully capture this.

Figure 8a plots time series of the NARR-forced surface energy balance terms, and Figures 8b-8d shows the relations between net energy and selected meteorological variables. ~~These are equivalent to the relations between total summer melt, and~~These provide a visual indication of the strength of each variable as a predictor of summer melt. Regressions through these data points give estimates of net energy sensitivity, e.g. ~~dQ_N/dT~~$\partial Q_N/\partial T$, as seen in actual realizations of the summer weather conditions. These ~~values~~gradients can be thought of as the melt sensitivity to interannual variability or trends in each weather variable.

The resulting sensitivities are given in Table 6, as well as linear correlation ~~values~~coefficients between Q_N and all glaciometeorological variables that are used in the energy balance model. These simulations are forced with NARR radiation flux anomalies, so we do not parameterize the incoming longwave or shortwave radiation in these tests. The clearness index, τ, is not used, but it can be calculated from the NARR relative humidity estimate, via Eq. (10), or more directly through the fraction of incoming shortwave radiation relative to the clear-sky potential radiation. We test both approaches and find similar results. Values for $\partial Q_N/\partial \tau$ reported in Table 6 are averaged from the two approaches. We also report the direct relation between NARR total cloud cover and net energy; cloud cover is available in the reanalysis, but we do not have *in situ* data to compare with.

Temperature and albedo have the strongest influences on summer energy balance and melt~~, while incoming longwave radiation and~~. Fluctuations in specific humidity ~~also emerge as significant influences on~~and incoming longwave radiation also correlate strongly with interannual variability in the summer energy budget. ~~Other variables, including~~Wind speed, cloud conditions, and incoming shortwave radiation~~,~~ do not strongly contribute to the year-to-year variations in summer melt over the NARR period. There is a weak, positive relationship between the clearness index and net radiation in the NARR-forced results, indicating that increased shortwave radiation associated with reduced cloud cover has a stronger role than the associated reduction in longwave radiation.

These sensitivities can be compared with those in ~~Sections~~Section 5 ~~that include full albedo and atmospheric radiation feedbacks,~~(Table 4), but they differ in that the NARR forcing has multiple joint perturbations. This is realistic as the meteorological variables ~~often~~ co-vary systematically, but it means that it is not possible to isolate the role of a single variable, such as temperature. A temperature change impacts several of the energy fluxes, but coincident changes in, e.g~~.~~., humidity and radiation fluxes, may reinforce or reduce the temperature impacts. ~~The results~~Results in Table 6 should therefore be interpreted as the 'net' or 'effective' influence of each weather variable on the summer energy balance, and some of them ~~(e.g., relative humidity)~~ may have correlations that are more coincidental than casual. —Most results are nonetheless similar in magnitude to the theoretical and modelling results (Tables 3 and 4), which are based on the *in situ* data. The largest exception is the relation between clearness index (cloud cover) and net energy, which is opposite in sign.

Formatted: Normal

7. Discussion

We ~~take~~have taken three different approaches to estimate summer (JJA) energy balance and melt sensitivity at Haig Glacier~~ in the Canadian Rocky Mountains~~: (i) theoretical, perturbing one ~~meteorological~~ variable at a time~~ with reference to the mean meteorological conditions~~, (ii) ~~through~~ a numerical model~~ of the surface energy balance~~, restricting model experiments to single perturbations but allowing for internal feedbacks to be modelled, and (iii) through ~~reanalysis-based meteorological~~ perturbations from a regional climate reanalysis, allowing multiple variables to change at once~~ in a way that is meteorologically consistent. The latter also permits a longer time period to be modelled (36 years), to examine~~. Here we briefly summarize and interpret the ~~role of~~integrated results from these different ~~meteorological variables in interannual variability of glacier melt.~~ methods.

~~In all three approaches to assess the sensitivity, perturbations in~~ *Haig Glacier Energy Balance Sensitivities and Feedbacks*

Formatted: Font: Italic

Interannual variations in temperature and albedo have the strongest influence on summer ~~melt extent.~~energy balance in all three approaches to assessing Haig Glacier melt sensitivity (Figure 9). Fluctuations in humidity and ~~incoming shortwave and~~ longwave radiation~~, via cloud cover,~~ are also important~~ to the summer energy budget~~, while variations in cloud cover (τ), wind speed, and the winter snowpack thickness are less influential on the summer energy budget and melt extent at this site. ~~We discuss each weather variable in a more detail in the next paragraphs.~~

~~*Temperature Perturbations*~~

Temperature changes are generally thought of as the main driver of glacier advance and retreat, through ~~various~~combined influences on the surface energy budget, snow accumulation, and summer melt season. ~~Numerous studies have estimated glacier melt or mass balance sensitivity~~Sensitivities to ~~climate warming. These sensitivities~~temperature are commonly expressed as the change in summer or net mass balance per unit warming. Sample mass balance sensitivities reported in the literature are –0.6 m w.e. °C^{-1} on Morteratschgletscher, Switzerland (Klok and Oerlemans, 2004) and Illecillewaet Glacier, British Columbia (Hirose and Marshall, 2013), –0.68±0.05 m w.e. °C^{-1} for a suite of glaciers in Switzerland (Huss and Fischer, 2016), and –0.86 m w.e. °C^{-1} on South Cascade Glacier, Washington (Anslow et al., 2008). Values as high as –2.0 m w.e. °C^{-1} are reported for Brewster Glacier, New Zealand (Anderson et al., 2010).

These values are for the annual mass balance, but they are dominated by the summer melt response to warming~~, and they~~. They represent a melt sensitivity of about 30% °C^{-1} for the examples in the Alps and western North America. When we introduce temperature perturbations in the absence of albedo feedbacks, we find a relatively muted energy balance response, about ~~+10 W m^{-2}~~13 % °C^{-1} ~~averaged over~~. The increase in net energy is distributed about equally across the ~~main summer melt season, JJA. This equates to a melt~~sensible heat flux, incoming longwave radiation, and latent heat flux, and we have similar results for both the theoretical and numerically-modelled temperature perturbations. Albedo feedbacks increase the net energy sensitivity ~~of about 10~~to 28 % °C^{-1} ~~at this site,~~ or –0.~~2~~66 m w.e. °C^{-1}~~.~~, in accord with previous studies. The exact number depends on~~ the~~ assumptions about humidity; if specific humidity increases with temperature (e.g., by holding relative humidity constant), temperature sensitivity is higher. ~~This idealized warming is distributed about equally across the sensible heat flux, incoming longwave radiation, and latent heat flux, and we have the same result for both the theoretical and numerically-modelled temperature perturbations.~~

~~When~~The albedo ~~feedbacks are activated in our model, the impacts of a~~feedback results from two main ways that temperature ~~change are amplified dramatically at this site: roughly a five-fold increase in the melt sensitivity, to ~50% °C^{-1}. This is equivalent to about –1.2 m w.e. °C^{-1}. The~~

~~relationship is nonlinear and is strongest near the observed present-day temperature. Several effects can contribute to this strong amplification of the temperature signal in the melt model. A longer and~~influences the seasonal albedo evolution. A more intense melt season gives rise to a lower ~~albedo through higher impurity concentration and water content~~snow albedo and an earlier transition from seasonal snow cover to glacial ice.~~ These positive feedbacks also operate (in reverse) under a cool perturbation.~~ We do not explicitly model impurities or snow-albedo processes (e.g., grain metamorphosis, effects of snow-water content on the albedo), but we parameterize the seasonal albedo evolution as a function of cumulative *PDD* (Eq. ~~20). This is a rough proxy for cumulative melt effects that lower the albedo, and is empirically supported, but positive degree days are a direct function of temperature so this may make our albedo model overly~~20), which makes the model directly sensitive to temperature perturbations.

Temperature changes have several additional, indirect impacts, including: (i) a longer melt season~~, starting earlier and ending later~~, (ii) a greater fraction of time with surface temperatures at the melting point during the year, i.e., with reduced overnight cooling and refreezing, and (iii) an increase in the frequency of summer rain vs. snow events. Summer snow events have an important impact on surface albedo, with fresh snow strongly attenuating melt. Each of these processes contributes to the strong impact of ~~increased temperatures~~temperature anomalies on glacier melt. Combined with the albedo feedbacks, these processes and ~~the model results~~ help to explain why glaciers are ~~so~~strongly sensitive to temperature change~~, as they clearly are in natural settings (e.g., Marzeion et al., 2014).~~.

~~When multiple meteorological perturbations are introduced at the same time, in the NARR-based surface energy balance modelling, interannual temperature fluctuations appear to be weaker than the sensitivity experiments would suggest, ~14% °C^{-1}, although mean summer net energy and temperature are highly correlated (r = 0.84). All feedbacks discussed above are active in the NARR-based simulations. The impacts of temperature variability on net energy and melt could be partially compensated by other systematic changes in the energy budget. For instance, warm temperatures could be associated with calm, dry conditions that reduce the incoming longwave radiation and the turbulent fluxes. NARR mean summer temperature over the 36-year period is negatively correlated with wind speed (r = –0.11) and cloud cover (r = –0.50), which supports this possibility.~~

~~*Albedo Perturbations*~~

Direct changes to albedo have an influence on summer energy balance and melt extent that is comparable to the temperature influence~~. The three different methods of gauging albedo sensitivity give similar results, a summer energy balance impact of 22-26 W m^{-2}~~, ~17% for a change in albedo ~~of 0.1 (Tables 3, 4 and 6). Interannual albedo fluctuations are associated with net energy and melt variations of about 12%, a large fraction of the interannual variability.~~

equal to the interannual albedo fluctuations, 0.06. Mean summer albedo differences arise as a feedback to other meteorological forcings that drive the summer ~~snowpack evolution, such as temperature. Interannual~~snow melt, but interannual albedo variations ~~can~~ also occur more directly, as a consequence of ~~frequent~~ summer snowfall events~~ or~~, as a ~~result~~function of ~~low or high~~ winter accumulation totals, ~~which influence how long the seasonal snowpack will persist through the~~

~~summer. Haig Glacier is also vulnerable~~or due to impurity loading (e.g., black carbon deposition~~)~~). The latter has been observed in association with forest fires in British Columbia. ~~Extensive~~Strong fire seasons ~~have~~ occurred twice during ~~the~~our period of study~~ at this site,~~, in 2003 and 2015, and each left a ~~visibly and~~ measurably darker glacier surface. For instance, the average albedo recorded at the AWS site in August 2003 was 0.13.

~~*Humidity Perturbations*~~

~~Changes in humidity directly affect the latent heat flux, but they also influence the incoming radiation fluxes in our parameterizations, through the atmospheric emissivity and the clearness index. Net energy has~~ We found a ~~large unit sensitivity to specific humidity, but interannual variability at the site is~~ relatively ~~low, such that fluctuations in specific humidity do not strongly influence summer melt extent. This is true for both the observational period and in the NARR-forced reconstructions.~~

~~Mean summer latent heat flux was weakly negative through the observational period at the Haig Glacier AWS site, but increases in specific humidity increase this flux and it switches signs to a small positive flux with a 5% (~0.2 g kg^–1^) increase in JJA humidity. Radiation fluxes are more strongly sensitive to humidity, at least as parameterized in our study, with relative humidity being the main influence. Atmospheric emissivity and incoming longwave radiation increase with humidity, while incoming shortwave radiation is reduced, based on the empirical link between relative humidity and cloud cover. These fluxes largely compensate and offset each other, but the longwave radiation has a stronger response in our results, for both the theoretical and modelled perturbations in humidity. There is a net cooling influence when specific humidity is reduced, as decreases in incoming longwave radiation exceed the attendant increases in shortwave radiation. Increases in humidity give an increase in net radiation, as gains in incoming longwave radiation again exceed the reductions in net shortwave radiation. The balance will depend on the surface albedo, which reduces the magnitude of shortwave radiation anomalies in the net energy budget.~~

~~*Incoming Shortwave Radiation*~~

~~Top-of-atmosphere shortwave radiation fluctuations, i.e. solar variability, have only minor influences on glacier melt, as top-of-atmosphere forcing is diminished through atmospheric extinction and the glacier surface albedo. Fluctuations of ~3 W m^–2^ are attenuated to 1 W m^–2^, which is negligible relative to the daily and interannual variability associated with cloud cover.~~

~~The latter does have a significant impact on year-to-year melt conditions. Surface-level interannual variability in shortwave radiation forcing equates to fluctuations of about 6 W m^–2^ (6%) of the JJA net energy budget, and can compound the effects of warm temperatures in associated with hot, dry, clear-sky periods on the glacier. This is empirically borne out at the site, but shortwave radiation fluctuations are less important in the NARR-driven energy balance than they are in the observations. NARR shortwave radiation variations correlate positively but weakly with summer melt, and interannual variability of incoming shortwave radiation is muted in the reanalysis. The NARR dataset may not be picking up some of the persistent ridging conditions which are observed to drive strong summer melt events at the site.~~

~~*Winter Mass Balance*~~

~~We found only a minor~~weak influence of winter mass balance on the summer melt extent~~, based on observed interannual variability in winter snow accumulation as well as sensitivity experiments.~~ . A low snowpack depth has a greater impact, through an earlier transition to low-albedo bare ice. A deep winter snowpack has the opposite influence, supporting a higher average summer albedo, but the influence is weaker because the AWS site is in the upper ablation area, where the seasonal snowpack persists until late summer in most years. The effects of greater winter accumulation plateau once there is enough snow to survive the summer; beyond this point, additional snow has no effect on the summer albedo or melt extent. Sensitivity to winter mass balance would likely be stronger at lower altitudes on the glacier, and for the overall glacier mass balance.

~~*Multivariate Perturbations*~~

~~Meteorological variables do not vary as idealistically as in the simple experiments presented in this paper. In reality, meteorological variables all vary at once, and different weather systems will have tendencies for the combined meteorological perturbations to compensate (buffer) or accentuate (amplify) impacts on energy balance and melt. This is implicit in the NARR-forced simulations, which sample a 36-year record of interannual variability with physically-consistent covariance of meteorological variables.~~

Humidity changes can also be considered a feedback to temperature, but this is not certain; specific humidity varies as a function of local- to synoptic-scale moisture sources and weather patterns, and these are not necessarily coupled to temperature conditions. For instance, warm conditions at Haig Glacier often accompany anticyclonic ridging in the summer months, during which time southerly flows and upper-level subsidence promote dry, clear-sky conditions (low q_v and h). At other times, westerly flows bring warm, moist Pacific air masses and humidity, temperature, and cloud cover co-vary. Interannual variability in specific humidity has a significant impact on summer energy and melt extent, an ~8% change for a perturbation of 0.3 g kg^{-1} (1σ). This effects net energy through impacts on the latent heat flux and incoming longwave radiation. The latter is partially compensated by accompanying changes in incoming shortwave radiation.

With all three methods, cloud cover shows up as a relatively weak influence on summer net energy at this site, ~4% for a 1-σ variation in the clearness index (Figure 9). This result is a consequence of the offsetting effects of cloud cover on the shortwave and longwave fluxes. The sign of the relationship is also uncertain. In isolation, interannual fluctuations in shortwave and longwave radiation have a moderate influence on the summer net energy (Figure 9), so these are important; they are just not simply related to the cloud cover index, τ.

NARR Results

NARR results are broadly consistent with the ~~idealized experiments~~*in situ*-based and theoretical sensitivities, in terms of the relative importance of different meteorological parameters to interannual variability in summer energy balance and melt. The influence of interannual temperature fluctuations appear to be weaker than the other sensitivity experiments would suggest, ~15% °C^{-1}. All feedbacks discussed above are active in the NARR-based simulations. The impacts of temperature variability on net energy and melt could be partially compensated by other systematic changes in the energy budget. ~~The~~For instance, warm temperatures are often associated with calm, clear-sky conditions that reduce the incoming longwave radiation and the turbulent fluxes.

Temperature nonetheless emerges as the most important variable explaining interannual variations in net energy. Mean summer net energy and temperature are highly correlated (r = 0.84). This reinforces the argument that temperature indices offer a good proxy for net energy and summer melt extent (e.g., Ohmura, 1987).

There are two ~~main~~other discrepancies ~~are that the temperature sensitivity and year~~in the NARR-forced results. Year-to-year variance in incoming ~~shortwave radiation are less than expected. This may be connected, as the highest observed summer mass losses have occurred in hot, dry summers, where there were strong positive anomalies in both shortwave radiation and temperature. We do not~~radiation fluxes is less than observed, pointing to poor representation of interannual cloud variability in the reanalysis. The variability is still positively correlated with the in situ data (e.g., r = 0.50 for the correlation between incoming JJA shortwave radiation in NARR and in the data from 2002-2012). Hence, NARR is picking up some of the observed variability, but it is muted. The sensitivities to the radiation fluxes may still be representative, as there is still some interannual variability for which on can assess the relation between Q_N and the radiation fluxes. However, the poor representation of the radiation fluxes and cloud conditions can be expected to reduce the skill of NARR-forced mass and energy balance reconstructions; this requires further study.

The other main difference with the NARR forcing is a switch in sign in the sensitivity to changes in cloud cover, as analyzed through either τ or the NARR-predicted total cloud cover. Clear-sky conditions have a positive relation with Q_N in the NARR-driven simulations, signalling that incoming shortwave radiation fluxes exert more influence than incoming longwave fluxes for net summer energy. Clear-sky conditions (less cloud cover) give increased shortwave radiation and a lesser decrease in longwave radiation, resulting in increased net energy. The theoretical and *in situ* sensitivities predict the opposite result, reduced net energy with clearer skies. The relationship is relatively weak, so it is possible that there are confounding variables in the NARR simulations once again, such as temperature effects masking the cloud relationship.

We do not test the ability and skill of NARR-forced energy and mass balance reconstructions here. This requires further study. In general, the perturbation method eliminates biases in the mean NARR variables, but a realistic representation of the variability and long-term trends in reanalysis fields is important to realistic representations of the glacier mas balance record and meltwater runoff. It would be instructive to analyze the synoptic weather patterns and weather anomalies in high-melt vs. low-melt summers in the NARR-driven simulations. ~~An~~We recommend an investigation of specific weather systems and their associated meteorological and energy balance conditions ~~is recommended for~~in followup work.

~~Daily NARR-based forcings for the surface energy balance and summer melt/mass balance worked well in this study, when taken as anomalies to the mean observed conditions. This method for calculating the surface energy balance is a general approach that can be adopted to explore meteorological influences on melt in different glacier environments, or to model variations in time~~

~~at a particular site. The method could similarly be applied to climate model output for future projections.~~

Representativeness of the Results

We have designed the sensitivity approach and the model to be applicable in regional studies, e.g. in a distributed model of glacier energy balance, forced by climate model reanalyses or projections. However, we did not expand our scope to other sites within the present study. In principle, the theoretical sensitivities (i.e. from the same set of equations) could be calculated for different baseline meteorological conditions, such as maritime or tropical environments. The method, rather than the specific Haig Glacier results, could be exported to other glacierized environments.

At regional scales, Haig Glacier energy balance sensitivities might be more transferrable, since similar summer climate conditions prevail across the Canadian Rocky Mountains (Ebrahimi and Marshall, 2015). Regional, multi-year reconstructions of glacier meltwater runoff might be feasible through a perturbation approach to summer mass balance, driven by meteorological anomalies from station data or climate models. This needs to be tested, however, for sensitive parameterizations such as the albedo model. It is uncertain whether the Haig glacier bare-ice and old-snow albedo are regionally representative.

Within Haig Glacier itself, our AWS site is in the upper ablation area, near the equilibrium ELA. Results are specific to the snow and ice albedo, snowpack depth, and meteorological/energy balance conditions at this location. We have not examined the representativeness of the results to other parts of the glacier, but summer melt extent and mass balance at the AWS site are strongly correlated with glacier-wide mass balance. We recommend additional work to calculate an average set of glacier sensitivities and assess whether the values presented here are representative. We suspect that sensitivity of net energy to winter snow depth and the strength of albedo feedbacks will vary across the glacier.

Recommended Model Improvements

Model improvements are ~~certainly possible, particularly~~recommended with respect to our treatment of the glacier surface albedo and precipitation modelling.~~ Based on our systematic underestimation of September albedo, a better treatment of late-summer snow accumulation and the transition to the winter accumulation season is needed.~~ The energy balance, albedo, and melt models perform well in the core summer melt season, June through August, when summer snowfall is infrequent and impacts on the albedo are transient. We systematically underestimate September albedo, however; better treatments of late-summer snow accumulation and the transition to the winter accumulation season are needed.

Our meltwater drainage model is also simplistic. We assume that water drains efficiently from the glacier surface, but in fact water has been observed to pond and refreeze ~~here. This acts as an energy sink and would reduce~~on the surface. Re-melting ~~and~~of this superimposed ice consumes energy and reduces the total summer runoff~~ from the site~~.

A more realistic treatment of year-round snow accumulation is also needed in order to carry out model-based glacier mass balance reconstructions. We rely on observed winter mass balance for the studies here, but historical reconstructions and future projections require a way to reliably estimate snow accumulation from climate models. NARR precipitation in the Haig Glacier grid cell poorly represents the observed winter accumulation totals.

We have done tests to verify that the daily, parameterized model performs well relative to direct forcing with 30-minute AWS data, but some simplifications embedded in the daily model need to be examined. For instance, we assume constant cloud cover/clearness index over the day; systematic diurnal variations in cloud cover would affect the net radiation in ways that we do not capture. Overnight clouds serve to increase energy flux to the glacier, while daytime clouds reduce the incoming radiation. Effects like these become complicated to model or parameterize, but could bias our sensitivity results to cloud cover.

8. Conclusions

~~Theoretical~~Sensitivity studies presented here extend the foundational work of Oerlemans and ~~numerical models exploring surface energy~~ Fortuin (1992) and others, which has generally been done on glacier mass balance ~~on Haig Glacier~~sensitivity to changes in ~~the Canadian Rocky Mountains provide~~temperature and precipitation. Our study is limited to summer mass balance at one location, but our results offer insight into ~~summer melt sensitivity to~~ the influence of different meteorological variables and energy fluxes, their year-to-year variability, and the role of isolated vs. collective forcings~~. The study is based on a 11-year record of glaciometeorological conditions from an AWS site in the upper ablation area, 2002-2012. Numerical experiments examine perturbations to variables in isolation, with internal~~, feedbacks ~~to the~~, and interactions on summer melt ~~season evolution, and with multiple perturbations to meteorological variables,~~extent.

There is a good correspondence between the theoretical sensitivities and those derived from ~~North American Regional Reanalyses from 1979-2014.~~ the numerical energy balance model, when feedbacks are omitted. This supports the potential application of the theoretical sensitivities to explore energy balance sensitivities under different climate regimes. This method can be transferred directly to other sites.

~~The model runs year-round, to simulate sub-surface temperature evolution in the winter snowpack and to include the complete summer melt season (May to September), but our analysis concentrates on mean summer (JJA) surface energy balance and melt. Just over 80% of the annual melt at the site occurs in JJA, and we find similar energy balance and melt sensitivity to meteorological variability when we look at MJJAS.~~

Temperature and albedo variations exert the strongest controls on year-to-year variability in summer melt at our site. While albedo can fluctuate independent of temperature, e.g., through the influence of the winter snowpack depth or aerosol loading, it is also a powerful feedback mechanism to temperature and melt season evolution. In our model, albedo feedbacks give a ~~five~~two-fold increase in the net energy balance sensitivity to a temperature perturbation, amplifying the summer melt response from ~~10~~13% °C^{-1} to ∼~~50~~28% °C^{-1}. Temperature and albedo

Formatted: Font color: Text 1

Formatted: Font color: Text 1

Formatted: Font color: Text 1

Formatted: Font color: Text 1

Formatted: Font color: Text 1

Formatted: Font color: Text 1

Formatted: Font color: Text 1

Formatted: Font color: Text 1

fluctuations are also the strongest influences on interannual melt variations in the NARR-forced surface energy balance, but the melt sensitivity to temperature variations is about 15% °C^{-1}, weaker than our result from the control experiments. This may be because the co-variation of other variables in the surface energy balance partially offsets the temperature forcing. ~~For example, temperature increases are associated with lower relative humidity and cloud cover, which reduces incoming longwave radiation. It is also possible that NARR climate reconstructions are not adequately capturing the weather conditions and their interannual variability over the field site, as suggested by a poor representation of cloud conditions and radiation fluxes compared to in situ observations.~~

~~Other meteorological variables cannot be neglected in the surface energy balance and its interannual variability. At Haig Glacier, incoming shortwave radiation fluctuations are particularly influential on summer melt extent. The strongest melt seasons and most negative mass balance years on record at the site, 2003, 2006, and 2015 (not shown), were each associated with persistent anticyclonic ridging in the summer months, giving warm, dry, clear-sky conditions, i.e. co-variance of strong positive anomalies in temperature and incoming shortwave radiation.~~

Humidity fluctuations are also effective in influencing the net energy, through their impacts on latent heat flux and incoming radiation fluxes. Wind speed, cloud conditions, and the winter snowpack thickness are less important to the summer energy balance and melt extent at our site. The relationship with cloud conditions is statistically weak and we do not have confidence in the sign; we recommend further work to assess the influence of cloud cover on summer net radiation at this site and elsewhere.

~~These~~Our results ~~apply to just one location, in the upper ablation area of a relatively small~~suggest that it is may be reasonable to model glacier~~. While this is a typical mid-latitude mountain glacier, other parts of the glacier (i.e. the lower ablation zone) and other glaciers will have different energy balance sensitivities to meteorological conditions. This contribution is an initial step, introducing an energy balance~~ melt sensitivity ~~approach to quantify glacier sensitivity to meteorological~~at this site to temperature forcing, while ignoring variability and ~~climate~~ change~~. Further work is needed and recommended to extend this approach to different climate regimes.~~

~~Our analyses and results focus on the summer melt season; additional work is also needed to extend this to the broader implications for glacier mass balance, including winter mass balance and its sensitivity to meteorological variability and change. Winter snow accumulation is governed by synoptic~~ in other weather ~~and storm track patterns more than surface energy balance conditions, at least in the Canadian Rocky Mountains (e.g., Shea and Marshall, 2007; Sinclair and Marshall, 2009), so this is beyond the scope of the present study.~~

~~Sensitivity studies presented here extend the foundational work of Oerlemans and Fortuin (1992) and others, which has generally been done on glacier mass balance sensitivity to changes in temperature and precipitation. Our study is limited to summer mass balance at one location, but our results offer insight into the influence of different meteorological variables and energy fluxes, their year-to-year variability, and the role of isolated vs. collective forcings, feedbacks, and interactions on summer melt extent.~~

~~Results affirm the importance of temperature~~conditions such as ~~a driving variable in~~ wind speed and cloud cover. This is the implicit premise in temperature-index melt models, and they can be

Formatted: Font color: Auto

Formatted: Font color: Auto

Formatted: Font color: Auto

Formatted: Font color: Auto

tuned to work well at our site. We hesitate to recommend this though. Albedo feedbacks are crucial to include in assessments of glacier response to ~~climate change, amplified by numerous~~ temperature~~-related feedbacks in the melt season evolution. However,~~ change, and are not physically represented in most ~~variables that influence the surface energy balance have non-~~ temperature-index models. Variations in humidity and their influence on melt are not negligible ~~influences on~~, and all terms in the surface energy budget ~~and summer melt extent. Temperature-index methods of estimating melt neglect potentially important impacts from cloud cover, humidity, and the seasonal albedo evolution. Caution is needed when applying these methods to future projections.~~ contribute to the daily and interannual fluctuations in net energy.

Our modelling approach for surface energy balance is well-suited to a distributed energy balance model, applying the perturbation approach to larger scales (e.g., mountain ranges). Climate models simulate all of the relevant meteorological fields, and both past reanalyses and future projections can be driven using the perturbation approach introduced here. Meteorological sensitivities under different climate regimes (e.g., maritime, polar, or tropical conditions) can also be explored using this framework, to help understand ~~the~~regional differences in glacier sensitivity to climate variability and change~~ in different regions.~~ .

Formatted: Font color: Auto

Formatted: Font color: Auto

Formatted: Font color: Auto

Formatted: Justified

Acknowledgements

This contribution benefitted from detailed reviews and insights of two anonymous reviewers and the Editor. It is much-improved from the reviewers' suggestions. We thank the Natural Sciences and Engineering Research Council (NSERC) of Canada for long-term support of the Haig Glacier study. S. Ebrahimi is financially supported through NSERC and the Alberta Water Research Institute project Predicting Alberta's Water Future. We are indebted to numerous graduate students and research assistants who helped to collect data and maintain instrumentation at Haig Glacier since 2001.

References

Anslow, F.S., Hostetler, S., Bidlake, W.R. and Clark, P.U., Distributed energy balance modeling of South Cascade Glacier, Washington and assessment of model uncertainty. J. Geophys. Res.-Earth Surface., 113(F2), 2008.

Anderson, B., Mackintosh, A., Stumm, D., George, L., Kerr, T., Winter-Billington, A. and Fitzsimons, S.: Climate sensitivity of a high-precipitation glacier in New Zealand, J. Glaciol., 56(195), 114-128, 2010.

Andreas, E. L.: Parameterizing scalar transfer over snow and ice: a review, J. Hydrometeorol., 3, 417-432, 2002.

Arendt, A., Walsh, J. and Harrison, W.: Changes of glaciers and climate in northwestern North America during the late twentieth century, J. Climate, 22(15), 4117-4134, 2009.

~~Arnold, N. S., Willis, I. C., Sharp, M. J., Richards, K. S., and Lawson, M.J.: A distributed surface energy balance model for a small valley glacier. I. Development and testing for Haut Glacier d'Arolla, Valais, Switzerland, J. Glaciol., 42, 77-89, 1996.~~

Braithwaite, R.J. and Raper, S.C.: Glaciers and their contribution to sea level change, Phys. Chem. Earth, Parts A/B/C, 27(32), 1445-1454, 2002.

Braun, M. and Hock, R.: Spatially distributed surface energy balance and ablation modelling on the ice cap of King George Island (Antarctica), Global Planet. Change, 42, 45-58, 2004.

Brock, B. W., Willis, I. C., and Sharp, M. J.: Measurement and parameterisation of albedo variations at Haut Glacier d'Arolla, Switzerland, J. Glaciol., 46, 675-688, 2000.

Brutsaert, W.: On a derivable formula for long-wave radiation from clear skies, Water Resour. Res., 11, 742-744, 1975.

Campbell, F. M. A., Nienow, P. W. and Purves, R. S.: Role of the supraglacial snowpack in mediating meltwater delivery to the glacier system as inferred from dye tracer investigations, Hydrol. Process., 20, 969-985, 2006.

Clarke, G. K. C., Jarosch, A. H., Anslow, F. S., Radić V., and Menounos, B.: Projected deglaciation of western Canada in the twenty-first century, Nat. Geosci. 8, 372-377, 2015.

Colbeck, S. C.: The capillary effects on water percolation in homogeneous snow. Journal of Glaciology, 13(67), 85-97, 1974.

Cuffey, K. M., and Paterson, W. S. B.: The Physics of Glaciers, 4th Ed., Academic Press, Amsterdam, 2010.

Demuth, M.N., and Keller, R.: An assessment of the mass balance of Peyto Glacier (1966-1995) and its relation to recent and past-century climatic variability, In: Peyto Glacier: One Century of Science, National Hydrology Research Institute Science Report Series #8, Demuth, M.N., Munro, D.S., and Young, G.J., Environment Canada, Saskatoon, Sask., 83-132, 2006.

Dyurgerov, M.B.: Mountain glaciers at the end of the twentieth century: global analysis in relation to climate and water cycle, Polar Geog., 25(4), 241-336, 2001.

Ebrahimi, S., and Marshall, S. J.: Parameterization of incoming longwave radiation at glacier sites in the Canadian Rocky Mountains, J. Geophys. Res.-Atmos., in press, doi: 10.1002/2015JD023324, 2015.

Engelhardt, M., Schuler, T.V. and Andreassen, L.M.: Sensitivities of glacier mass balance and runoff to climate perturbations in Norway, Ann. Glaciol, 56(70), 79-88, 2015.

Favier, V., Wagnon, P., Chazarin, J. P., Maisincho L., and Coudrain, A..: One-year measurements of surface heat budget on the ablation zone of Antizana Glacier 15, Ecuadorian Andes, J. Geophys. Res.-Atmos. (1984-2012), 109, D18, doi: 10.1029/2003JD004359, 2004.

Gerbaux, M., Genthon, C., Etchevers, P., Vincent, C., and Dedieu, J. P.: Surface mass balance of glaciers in the French Alps: distributed modeling and sensitivity to climate change, Journal of Glaciology, 51, 561-572, 2005.

Giesen, R. H., Van den Broeke, M. R., Oerlemans, J., and Andreassen, L.M.: The surface energy balance in the ablation zone of Midtdalsbreen, a glacier in southern Norway: Interannual variability and the effect of clouds, J. Geophys. Res.-Atmos., 113, D21, doi:10.1029/2008JD010390, 2008.

Giesen, R. H., L. M. Andreassen, M. R. van den Broeke en J. Oerlemans: Comparison of the meteorology and surface energy balance on Storbreen and Midtdalsbreen, two glaciers in southern Norway. The Cryosphere, 2009, 3, 57-74, doi: 10.5194/tc-3-57-2009.

Greuell, W., and Smeets, P.: Variations with elevation in the surface energy balance of the Pasterze (Austria). J. Geophys. Res.-Atmos. (1984-2012), 106, D23, 31717-31727, 2001.

Hirose, J. M. R., and Marshall, S. J.: Glacier meltwater contributions and glacio-meteorological regime of the Illecillewaet River Basin, British Columbia, Canada, Atmos.-Ocean, 51, 416-435, doi:10.1080/07055900.2013.791614, 2013.

Hock, R.: Glacier melt: a review of processes and their modelling, Prog. Phys. Geog., 29, 362-391, 2005.

Hock, R. and Holmgren, B.: Some aspects of energy balance and ablation of Storglaciären, Sweden, Geografiska Annaler, 78A, 121-131, 1996.

Hock, R. and Holmgren, B.: A distributed surface energy-balance model for complex topography and its application to Storglaciären, Sweden, J. Glaciol., 51, 25-36, 2005.

Huss M. and Fischer M., Sensitivity of very small glaciers in the Swiss Alps to future climate change. Cryospheric Sciences. 2016:34.

Klok, E. J., and Oerlemans, J.: Model study of the spatial distribution of the energy and mass balance of Morteratschgletscher, Switzerland, J. Glaciol., 48, 505–518, 2002.

Klok, E. J. and Oerlemans, J.: Modelled climate sensitivity of the mass balance of Morteratschgletscher and its dependence on albedo parameterization, Int. J. Climatol, 24, 231-245, 2004.

Klok, E.J., Nolan, M. and Van den Broeke, M.R.: Analysis of meteorological data and the surface energy balance of McCall Glacier, Alaska, USA, J. Glaciol., 51(174), 451-461, 2005.

Lhomme, J. P., Vacher, J. J., and Rocheteau, A.: Estimating downward long-wave radiation on the Andean Altiplano, Agr. Forest Meteorol., 145, 139–148, 2007.

Liou, K.N.: An Introduction to Atmospheric Radiation, 2nd Ed. Academic Press, Amsterdam, 583 pp, 2002.

Marshall, S. J.: Meltwater runoff from Haig Glacier, Canadian Rocky Mountains, 2002–2013, Hydrol. Earth Syst. Sci., 18, 5181–5200, doi:10.5194/hess-18-5181-2014, 2014.

Marzeion, B., Cogley, J. G., Richter, K., and Parkes, D.: Attribution of global glacier mass loss to anthropogenic and natural causes, Science, 345, 919-921, 2014.

Mesinger, F., DiMego, G., Kalnay, E., Mitchell, K., Shafran, P.C., Ebisuzaki, W., Jovic, D., Woollen, J., Rogers, E., Berbery, E. H., and Ek, M. B.: North American Regional Reanalysis, Bull. Amer. Meteor. Soc., 87, 343-360, 2006.

Mölg, T., Cullen, N. J., Hardy, D. R., Kaser, G., and Klok, L.: Mass balance of a slope glacier on Kilimanjaro and its sensitivity to climate, International Journal of Climatology, 28, 881-892, 2008.

Oerlemans, J.: The mass balance of the Greenland ice sheet: sensitivity to climate change as revealed by energy-balance modelling. The Holocene, 1, 40-48, 1991.

Oerlemans, J. and Fortuin, J. P. F.: Sensitivity of glaciers and small ice caps to greenhouse warming, Science (New York, N.Y.), 258, 115-117, 1992.

Oerlemans, J., Anderson, B., Hubbard, A., Huybrechts, P., Johannesson, T., Knap, W.H., Schmeits, M., Stroeven, A.P., Van de Wal, R.S.W., Wallinga, J. and Zuo, Z.: Modelling the response of glaciers to climate warming, Clim. Dynam., 14(4), 267-274, 1998.

Oerlemans, J., and Klok, E. J.: Energy balance of a glacier surface: analysis of AWS data from the Morteratschgletscher, Switzerland. Arct. Antarct. Alp. Res., 34, 115-123, 2002~~.: Extracting a climate signal from 169 glacier records, Science, 308, 675-677, 2005~~.

~~Oerlemans, J., and Klok, E. J.: Energy balance of a glacier surface: analysis of AWS data from the Morteratschgletscher, Switzerland. Arct. Antarct. Alp. Res., 34, 115-123, 2002.~~

Ohmura: Physical basis for the temperature-based melt-index method. J. Appl. Meteor., 40, 753–761, 2001.

Ohmura, A.: New temperature distribution maps for Greenland. Zeitschrift für Gletscherkunde und Glazialgeologie., 23 (1), 1-45, 1987.

Oke, T.R.: Boundary Layer Climates, 2nd Ed, Psychology Press, New York, 435, 1987.

Radić, V., and Hock, R.: Regionally differentiated contribution of mountain glaciers and ice caps to future sea-level rise, Nat. Geosci., 4, 91-94, 2011.

Sedlar, J., and Hock, R.: Testing longwave radiation parameterizations under clear and over-cast skies at Storglaciaren, Sweden, The Cryosphere, 3, 75–84, doi:10.5194/tc-3-75-2009, 2009.

Shea, J. M. and S. J. Marshall. Synoptic controls on regional precipitation and glacier mass balance in the Canadian Rockies. International Journal of Climatology, 27 (2), 233-247, 2007.

Sicart, J. E., Hock, R., and Six, D.: Glacier melt, air temperature, and energy balance in different climates: The Bolivian Tropics, the French Alps, and northern Sweden, J. Geophys. Res., 113, 2008.

Sinclair, K. E. and S. J. Marshall. The impact of vapour trajectory on the isotope signal of Canadian Rocky Mountain snowpacks. J. Glaciol., 55 (191), 485-498, 2009.

Wagnon P. W., Ribstein, P., Francou, B., and Pouyaud, B.: Annual cycle of energy balance of Zongo Glacier, Cordillera Real, Bolivia, J. Geophys. Res., 104, 3907-3923, 1999.

Wagnon P. W., Sicart, J. E., Berthier, E., and Chazarin, J. P.: Wintertime high-altitude surface energy balance of a Bolivian glacier, Illimani, 6340 m above sea level, J. Geophys. Res., 108 (D6 4177), doi:10.1029/2002JD002088, 2003.

Willis, I. C., Arnold, N. S., and Brock, B. W.: Effect of snowpack removal on energy balance, melt and runoff in a small supraglacial catchment, Hydrol. Process., 16, 2721-2749, 2002.

WGMS: World Glacier Monitoring Service, Zurich, Switzerland. Glacier Mass Balance Bulletins (M. Zemp et al., Eds.), ICSU(WDS)/IUGG(IACS)/UNEP/UNESCO/WMO, data available at http://wgms.ch/gmbb.html, 2014.

Tables

Table 1. Mean monthly weather conditions ± one standard deviation at Haig Glacier, Canadian Rocky Mountains, May to September 2002-2012. Data are from automatic weather station measurements at an elevation of 2660 m, in the upper ablation zone of the glacier.

Month	T (°C)	h (%)	e_v (hPa)	q_v (g/kg)	P (hPa)	v (m/s)
May	−1.4 ± 1.1	73 ± 4	4.0 ± 0.4	3.4 ± 0.4	743.0 ± 2.4	2.8 ± 0.2
June	2.6 ± 0.9	73 ± 6	5.5 ± 0.5	4.6 ± 0.4	748.1 ± 1.4	2.6 ± 0.2
July	6.9 ± 1.4	62 ± 5	6.4 ± 0.4	5.3 ± 0.3	751.2 ± 1.6	2.8 ± 0.3
August	5.9 ± 1.1	64 ± 7	6.1 ± 0.4	5.1 ± 0.4	750.8 ± 1.4	2.5 ± 0.2
Sept	2.1 ± 1.8	71 ± 10	5.0 ± 0.4	4.2 ± 0.3	748.4 ± 1.8	3.0 ± 0.4
JJA	5.1 ± 0.8	67 ± 4	5.7 ± 0.4	4.8 ± 0.3	750.0 ± 1.1	2.6 ± 0.2
MJJAS	3.2 ± 0.7	69 ± 4	5.3 ± 0.3	4.3 ± 0.3	748.3 ± 1.4	2.7 ± 0.2

Table 2. Mean monthly surface energy balance terms ± one standard deviation at Haig Glacier, Canadian Rocky Mountains, May to September 2002-2012. Radiation fluxes and albedo values are from automatic weather station measurements and the turbulent fluxes and subsurface heat conduction are modelled from the AWS data. Fluxes are in W m^{-2} and melt totals are in m w.e.

Month	$Q_S{\downarrow}$	α_s	$Q_L{\downarrow}$	$Q_L{\uparrow}$	Q_H	Q_E	Q_C	Q_N	*melt*
May	249 ± 24	0.76 ± 0.04	258±12	299±4	7±4	−11±3	5±2	22±12	0.20±0.10
June	237 ± 23	0.70 ± 0.05	276±14	310±2	17±4	−5±4	3±1	56±21	0.45±0.16
July	240 ± 19	0.57 ± 0.06	275±8	313±1	38±9	1±5	1±1	109 ±27	0.88±0.21
August	205 ± 25	0.38 ± 0.07	273±11	312±1	32±7	−1±3	2±1	123 ±22	0.99±0.18
Sept	140 ± 30	0.59 ± 0.09	271±13	306±3	23±12	−6±3	3±2	42 ±21	0.34±0.16
JJA	227 ± 14	0.55 ± 0.06	275±6	312±1	29±3	−2±3	2±1	97 ±19	2.32±0.45
MJJAS	215 ± 17	0.60 ± 0.04	271±7	308±1	23±4	−4±3	3±1	71 ±15	2.86±0.59

Table 3. Surface energy balance sensitivity to meteorological perturbations over a melting glacier surface, from direct feedbacks only. Calculations are for mean JJA conditions at Haig Glacier. All energy flux perturbations are expressed in W m^{-2}~~, and~~. $\delta Q_{N\sigma}$ is the net energy perturbation for a 1-σ increase in the variable. The melt perturbation, δm_{σ}, has units of mm w.e., and is calculated assuming that $\delta Q_{N\sigma}$ holds for JJA (92 days).

Perturbation	$-\delta Q_S^{\downarrow}$	$\delta\alpha$	δQ_S^{net}	$\delta Q_L^{\downarrow}$	$-\delta Q_H$	$-\delta Q_E$	δQ_N	$\delta Q_{N\sigma}$	δm ~~(mm)~~$_{\sigma}$
δT = 1°C; δh=0	−0	0	−0	4.7	−4.2	−3.5	−12.4	−~~295~~9.9	236
δT = 1°C; $\delta q_v=\delta\tau=\delta\varepsilon_a=0$	−0	0	−0	4.0	−4.2	−0	−8.3	~~−196~~6.6	157
δT = 1°C; δq_v=0; $\delta\tau$, $\delta\varepsilon_a$	−22.6	0	−10.2	−7.8	−4.2	−0	−6.6	−~~156~~5.3	125
δq_v = 1 g kg^{-1}; $\delta\tau=\delta\varepsilon_a$=0	−0	0	−0	0	−0	−10.5	−10.5	~~−248~~3.2	76
δq_v = 1 g kg^{-1}; $\delta\tau$, $\delta\varepsilon_a$	−41.8	0	−18.8	24.1	0	−10.5	15.7	~~−373~~4.7	112
δv = 1 m s^{-1}	−0	0	−0	0	8.3	−1.4	6.9	~~164~~2.1	50
δQ_0 = 1 W m^{-2}	−0.6	0	−0.3	0	−0	−0	−0.3	~~−7~~	3
~~$\delta\tau$ =~~ $\delta Q_S^{\downarrow}$ = 10 W m^{-2}	10.0	0~~.05~~	~~18.~~ 4.5	0	0 ~~8.1~~	−0	4.5	6.3	150
$\delta Q_L^{\downarrow}$ = 10 W m^{-2}	0	~~−8~~0	0	10	0	0	10.0	6.0	143
$\delta\tau$ = 0.1 ~~−192~~	36.0	0	16.2	−19.6	0	−4.6	−8.0	−3.2	−76
$\delta\alpha_S$ = 0.1	−0	0.1	−22.7	0	−0	−0	−22.7	~~−539~~ −13.6	−323
~~1σ, all (JJA)~~	~~14.0~~	~~−0.06~~	~~20.8~~	~~0.8~~	~~5.6~~	~~7.5~~	~~−34.6~~		~~821~~
~~1σ, all (MJJAS)~~	~~17.0~~	~~−0.04~~	~~16.0~~	~~5.5~~	~~4.6~~	~~7.3~~	~~−33.5~~		~~1323~~

Formatted: French (Canada)

Formatted: Font: 10 pt

Formatted: Font: 2 pt

Formatted: Font: 2 pt

Formatted: Font: 2 pt

Formatted: Font: 2 pt

Formatted: Font: 2 pt

Formatted: English (United States)

Formatted: French (Canada)

Formatted: Font: 3 pt

Table 4. Net energy balance sensitivity to meteorological perturbations in the surface energy balance model, based on regressions to the sensitivity curves (cf. Figure 6). Also shown is the change in net energy associated with a 1-σ increase in each parameter, averaged over JJA.

Perturbation	*Sensitivity*	δQ_N for +1σ

1. $\delta T = \pm 2$°C; $\delta h = 0$; $\delta\alpha_S = 0$	$\partial Q_N/\partial T =$ ~~10~~13 W m^{-2} (°C)$^{-1}$	~~+8~~+10 W m^{-2}
2. $\delta T = \pm 2$°C; $\delta h = 0$	$\partial Q_N/\partial T =$ ~~55~~27 W m^{-2} (°C)$^{-1}$	+~~44~~21 W m^{-2}
3. $\delta T = \pm 2$°C; $\delta q_v = \delta\tau = \delta\varepsilon_a = 0$	$\partial Q_N/\partial T =$ ~~51~~21 W m^{-2} (°C)$^{-1}$	+~~41~~17 W m^{-2}
4. $\delta T = \pm 2$°C; $\delta q_v = 0$; $\delta\tau$, $\delta\varepsilon_a$	$\partial Q_N/\partial T =$ ~~43~~17 W m^{-2} (°C)$^{-1}$	+~~34~~13 W m^{-2}
5. $\delta q_v = \pm 50\%$; $\delta\tau$, $\delta\varepsilon_a = 0$	$\partial Q_N/\partial q_v =$ ~~9 W m^{-2} (g/kg)$^{-1}$~~	~~+3 W m^{-2}~~
~~6. $\delta q_v = \pm 50\%$; $\delta\tau$, $\delta\varepsilon_a$~~	~~$\partial Q_N/\partial q_v =$ 18~~15 W m^{-2} (g/kg)$^{-1}$	+5 W m^{-2}
6. $\delta q_v = \pm 50\%$; $\delta\tau$, $\delta\varepsilon_a$	$\partial Q_N/\partial q_v =$ 25 W m^{-2} (g/kg)$^{-1}$	+8 W m^{-2}
7. $\delta v = \pm 50\%$	$\partial Q_N/\partial v =$ ~~−8~~14 W m^{-2} (m/s)$^{-1}$	+~~2~~3 W m^{-2}
8. $\delta\tau = \pm 0.1$	$\partial Q_N/\partial\tau = -9$ W m^{-2} (0.1)$^{-1}$	~~8. $\delta Q_S^{\downarrow} = \pm 20$ W m^{-2}~~
	~~$\partial Q_N/\partial Q_S^{\downarrow} = 0.$~~4 W m^{-2} ~~(W m^{-2})$^{-1}$~~	~~+6 W m^{-2}~~
9. $\delta\alpha_S = \pm 0.1$	$\partial Q_N/\partial\alpha_S = -$~~22~~27 W m^{-2} (0.1)$^{-1}$	−16 W m^{-2}
10. $\delta b_w = \pm 1$ m w.e.	$\partial Q_N/\partial b_w = -12$ W m^{-2} (~~0.~~m w.e.)$^{-1}$~~)$^{-1}$~~	~~−13~~ −3 W m^{-2}

Table 5. Summer surface energy balance fluxes on Haig Glacier as forced by the North American Regional Reanalysis (NARR) daily weather fields, 1979-2014. NARR inputs are taken as perturbations to the mean observed values. Melt is in m w.e., and all fluxes have units W m^{-2}.

Period	$Q_S^{\downarrow}$	α_s	$Q_L^{\downarrow}$	$Q_L^{\uparrow}$	Q_H	Q_E	Q_C	Q_N	*melt*
JJA	227 ± 7	0.53 ± 0.~~04~~05	275±4	311±1	27±4	−3±3	2±1	95 ±14	2.28± 0.~~32~~42
MJJAS	215 ± 6	0.55 ± 0.~~03~~04	271±4	308±2	22±3	−5±3	3±1	73 ±10	2.~~95~~68± 0.~~38~~50

Table 6. Correlation and sensitivity of different weather variables to the mean summer (JJA) net energy flux, Q_N, for the NARR simulations, 1979-2014. 'cloud' is the NARR total cloud fraction.

Variable	*Correlation*	*Sensitivity*	δQ_N for +1σ
T (°C)	0.84	$\partial Q_N/\partial T =$ 14 W m^{-2} (°C)$^{-1}$	+10 W m^{-2}
~~h (%)~~	~~0.33~~	~~$\partial Q_N/\partial h = -2$ W m^{-2} (%)$^{-1}$~~	~~−6 W m^{-2}~~
q_v (g kg^{-1})	0.50	$\partial Q_N/\partial q_v =$ 25 W m^{-2} (g/kg)$^{-1}$	+7 W m^{-2}
v (m s^{-1})	−0.~~07~~00	$\partial Q_N/\partial v = -4$ W m^{-2} (m/s)$^{-1}$	−1 W m^{-2}
$Q_S^{\downarrow}$ (W m^{-2})	0.14	$\partial Q_N/\partial Q_S^{\downarrow} = 0.3$ W m^{-2} (W m^{-2})$^{-1}$	+2 W m^{-2}
$Q_L^{\downarrow}$ (W m^{-2})	0.64	$\partial Q_N/\partial Q_L^{\downarrow} = 2$ W m^{-2} (W m^{-2})$^{-1}$	+8 W m^{-2}
τ	0.25	$\partial Q_N/\partial\tau = 15$ W m^{-2} (0.1)$^{-1}$	+4 W m^{-2}
cloud	−0.19	$\partial Q_N/\partial c = -8.1$ W m^{-2} 0.1)$^{-1}$	−3 W m^{-2}

Formatted: Font: 2 pt

Formatted: French (Canada)

Formatted: Font: 12 pt

Formatted: Font: 11 pt

Formatted: Font: 4 pt

Formatted: Superscript

α_S	-0.83	$\partial Q_N/\partial \alpha_S = -26\ \mathrm{W\,m^{-2}}\ (0.1)^{-1}$	$-11\ \mathrm{W\,m^{-2}}$
b_w (m w.e.)	$-0.\cancel{05}15$	$\partial Q_N/\partial b_w = -3\ \mathrm{W\,m^{-2}}\ (\mathrm{m\ w.e.})^{-1}$	$-1\ \mathrm{W\,m^{-2}}$

Formatted: Font: 12 pt, Superscript

Formatted: Font: 6 pt

Formatted: Subscript

Formatted: Font: 12 pt, Superscript

Figures

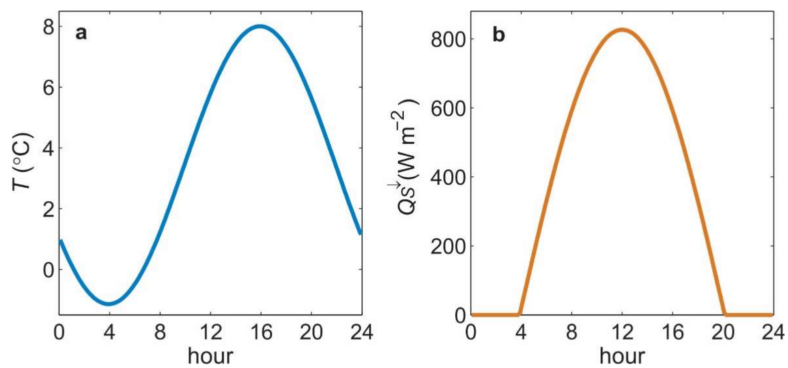

Figure 1. Idealized diurnal cycles of (a) temperature and (b) incoming shortwave radiation used in the energy balance model. These two examples are for a sample day, July 1, 2010, parameterized from daily minimum and maximum temperature in (a) and day of year plus mean daily incident shortwave radiation in (b).

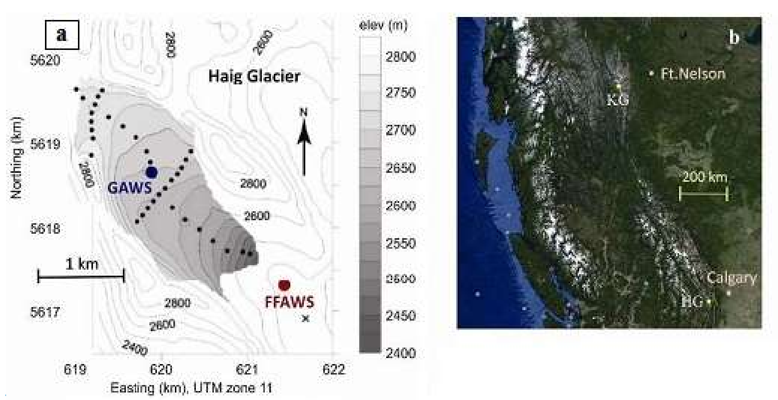

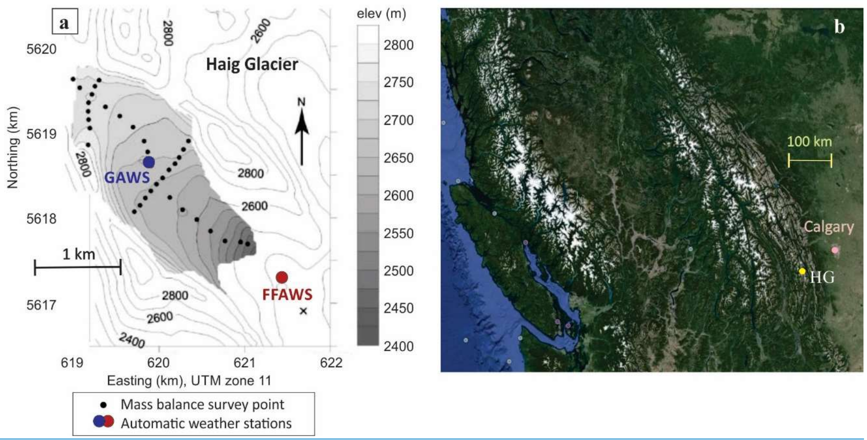

Figure 2. (a) The topography and automatic weather stations on Haig Glacier (GAWS) and the glacier forefield (FFAWS). The smaller black dots are mass balance survey points. (b) The location of Haig Glacier is labelled HG on the Google Earth map of ~~Western~~southwestern Canada.

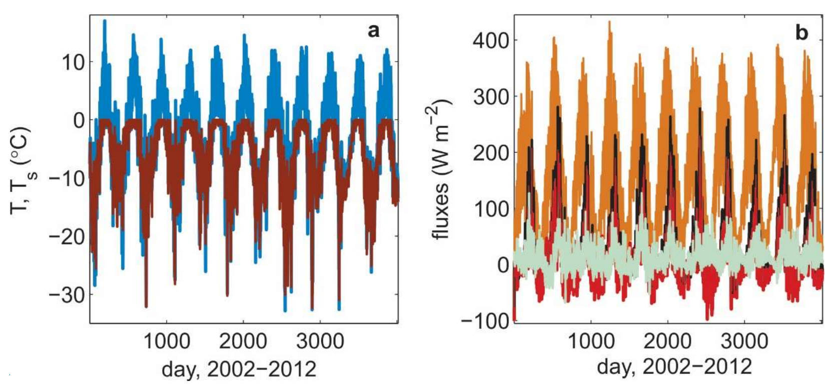

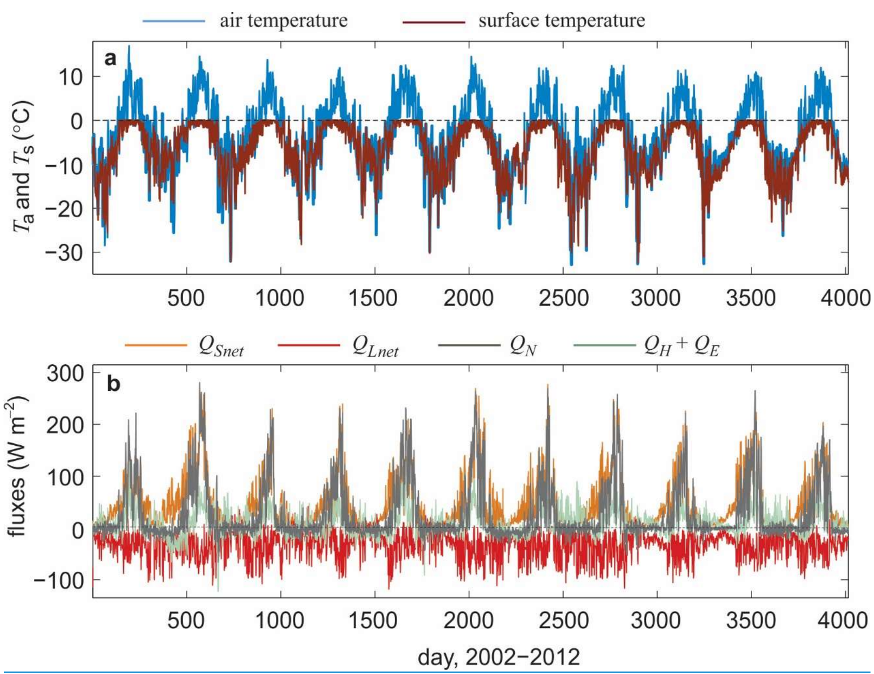

Figure 3. The 11-year record of (a) air temperature, modelled surface temperature, and (b) surface energy fluxes at the Haig Glacier AWS site. Daily mean values are plotted from Jan 1, 2002-Dec 31, 2012. ~~(a) Air temperature (blue) and modelled surface temperature (brown). (b) Incoming shortwave radiation (orange), net radiation (red), turbulent fluxes and Q_C (green), and net energy (black).~~

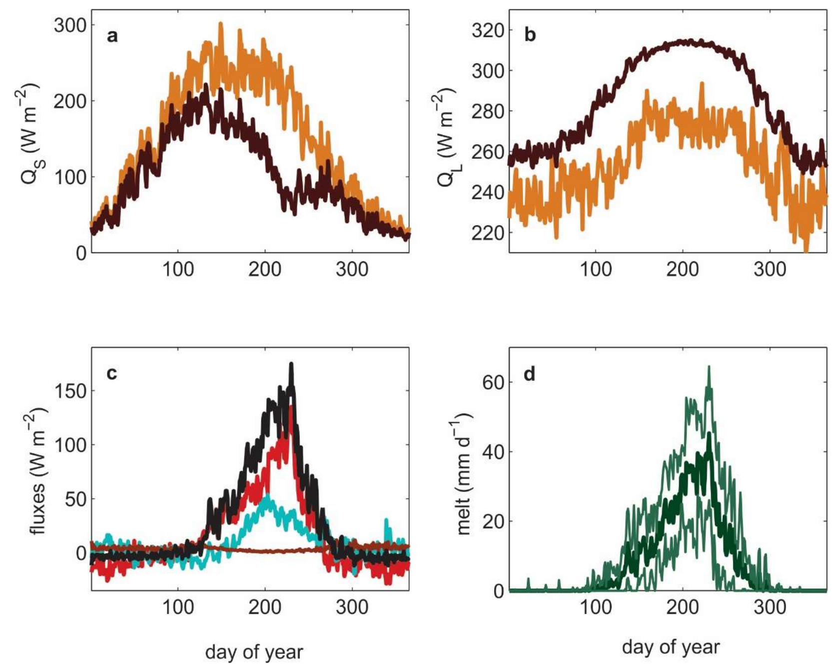
a
b
c
d
Q_S (W m^-2)
Q_L (W m^-2)
fluxes (W m^-2)
melt (mm d^-1)
day of year
day of year

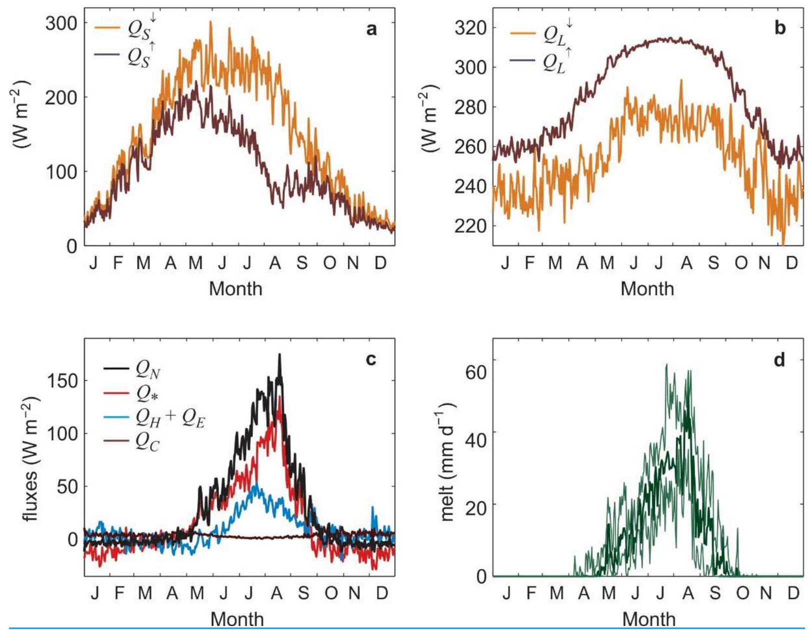

Figure 4. The average annual cycle of (a-c) surface energy fluxes and (d) daily melt at the Haig Glacier AWS. Daily mean values are plotted for the period 2002-2012. ~~(a) Incoming (orange) and outgoing (brown) shortwave radiation. (b) Incoming (orange) and outgoing (brown) longwave radiation. (c) Net radiation (red), turbulent fluxes (green), Q_C (brown), and net energy (black). (d) Melt~~For melt rates, ~~mm w.e. per day. The~~ the heavy line is the ~~11-year mean~~median value and the thin lines indicate the ~~mean ± 1 standard deviation~~interquartile range.

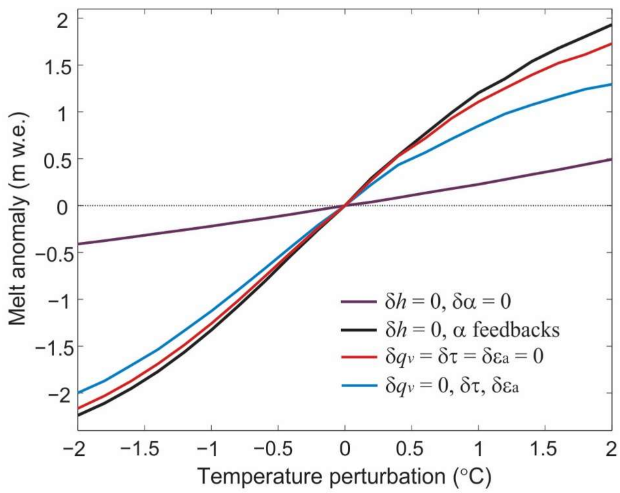

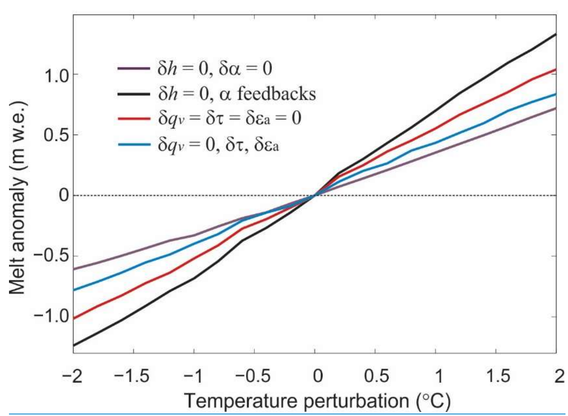

Figure 5. Sensitivity of modelled summer (JJA) melt to temperature perturbations for different assumptions, as per Table 4. ~~Purple line: relative humidity is constant, no albedo feedbacks.~~

~~Black line: relative humidity is constant, including albedo feedbacks. Red line: specific humidity is constant, no atmospheric feedbacks. Blue line: specific humidity is constant, including atmospheric feedbacks. The reference~~The reference (mean 2002-2012) JJA melt is 2.32 m w.e.

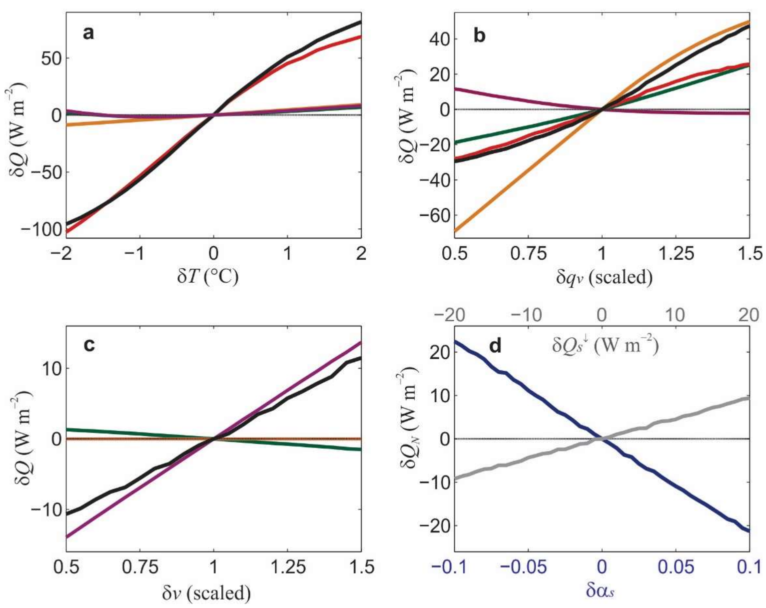

a
b
c
d
δQ (W m^-2)
δT (°C)
δqv (scaled)
δv (scaled)
δQN (W m^-2)
δQs↓ (W m^-2)
δαs

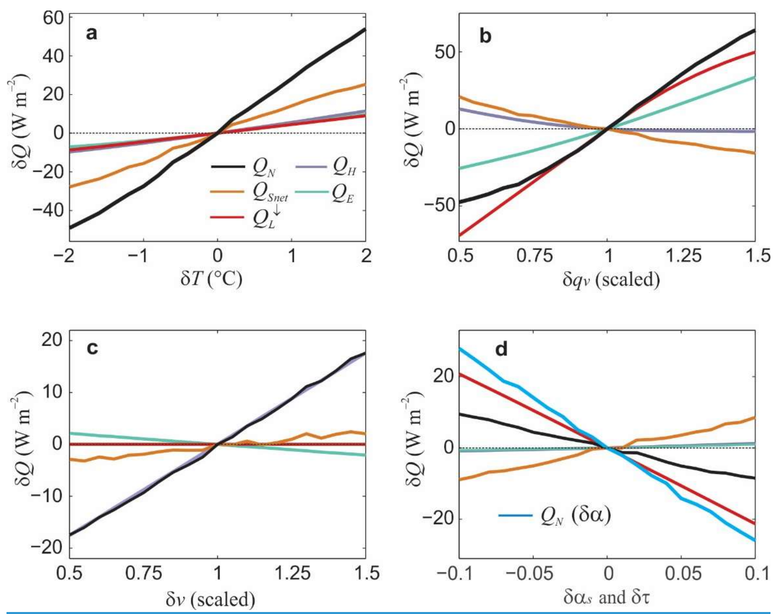

Figure 6. Sensitivity of the surface energy ~~balance~~fluxes at Haig Glacier to ~~a~~ changes in (a) temperature~~,~~ (case 2), (b) specific humidity~~,~~ (case 6), (c) wind speed~~,~~ (case 7), and (d) ~~shortwave radiation (grey~~atmospheric transmittance (case 8) and albedo (blue~~). For plots (a)-(c), black lines indicate the net radiation, purple lines are the sensible heat flux, green lines are the latent heat flux, red lines are the net radiation, and orange lines are the incoming longwave radiation.~~ line, case 9). All lines are anomalies relative to the baseline data from the period 2002-2012, and indicate the mean sensitivity of the different energy fluxes over this period. Please note the different y (δQ) scales.

Formatted: Centered

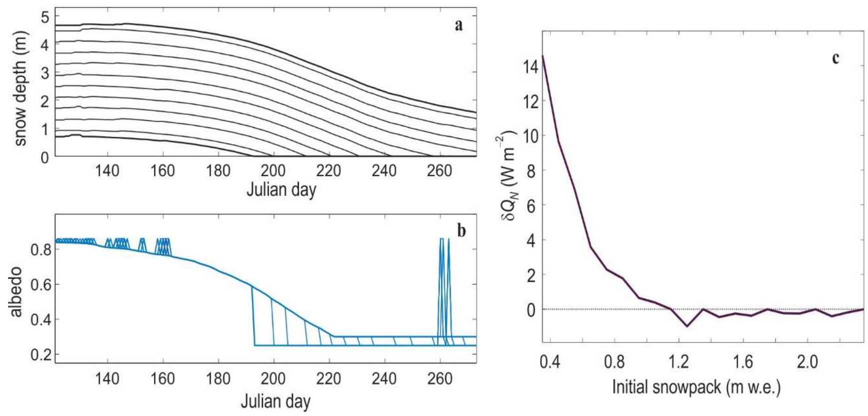

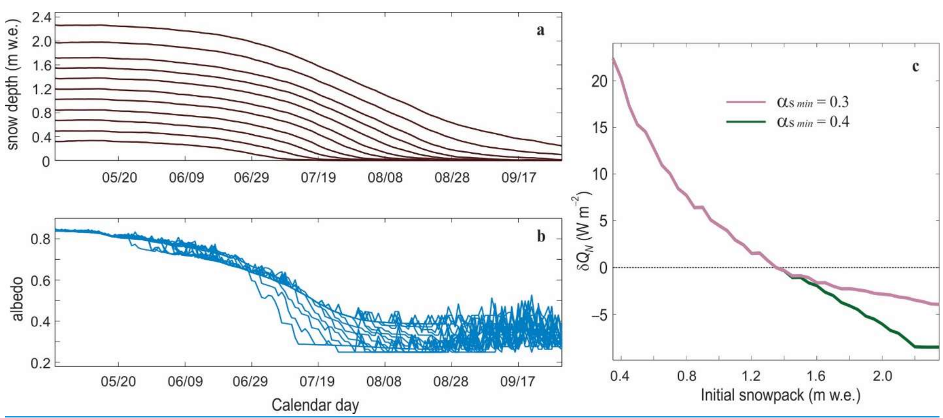

Figure 7. Sensitivity to the ~~initial snowpack (~~winter mass balance~~), for mean 2002-2012 weather conditions but with~~, examined by varying May 1 snow ~~varied~~depth from 0.~~35~~36-2.~~35~~36 m w.e., relative to the reference value of 1.~~35~~36 m w.e. at the glacier AWS. (a) Snow depth ~~(m)~~ and (b) albedo through the summer melt season, May 1-Sept 30, for the different ~~scenarios. Albedo spikes correspond to summer~~ initial snow ~~events~~depths. (c) Net summer (JJA) energy balance change as a function of the winter mass balance for two different settings of the minimum snow albedo.

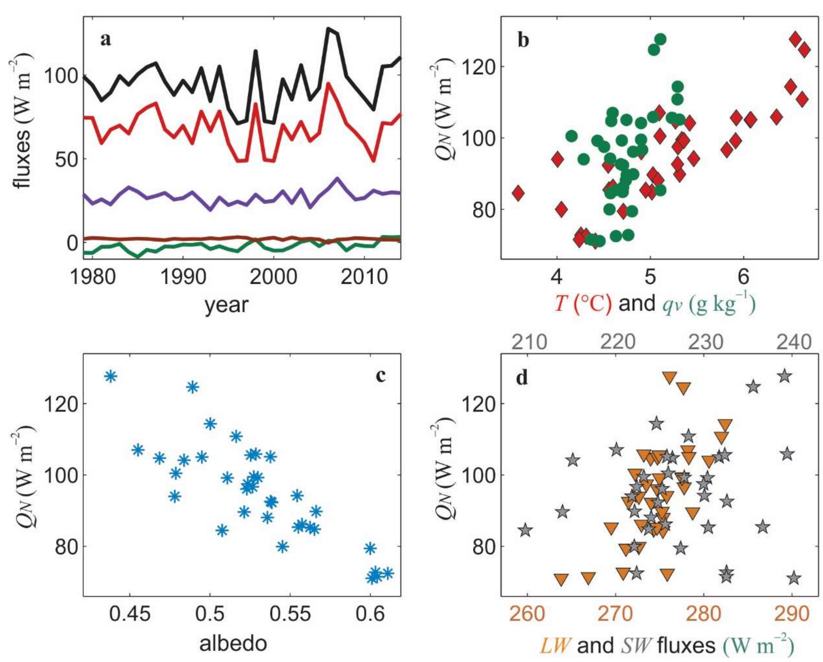
a
fluxes (W m^{-2})
100
50
0
1980
1990
2000
2010
year
b
Q_N (W m^{-2})
120
100
80
4
5
6
T (°C) and qv (g kg^{-1})
c
Q_N (W m^{-2})
120
100
80
0.45
0.5
0.55
0.6
albedo
d
210
220
230
240
Q_N (W m^{-2})
120
100
80
260
270
280
290
LW and SW fluxes (W m^{-2})

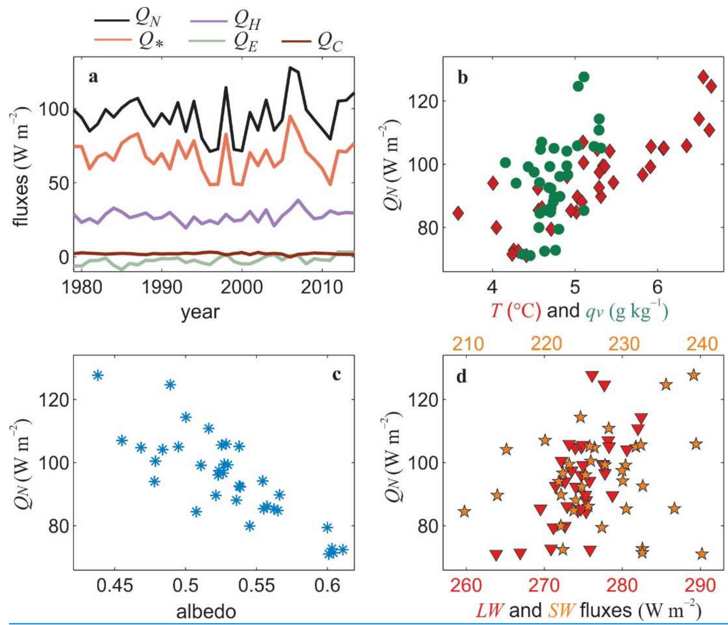

Figure 8. a) Mean summer (JJA) NARR-forced surface energy fluxes at Haig Glacier, 1979-2014. ~~Black: net energy. Red: net radiation. Purple: sensible heat flux. Brown: conductive heat flux. Green: latent heat flux. (b)~~ Mean summer net energy as a function of (b) temperature ~~(red diamonds)~~ and specific humidity~~ (green circles).~~, (c) ~~Mean summer net energy as a function of~~ albedo~~.~~, and (d) ~~Mean summer net energy as a function~~ incoming shortwave ~~radiation (grey stars) and incoming~~ and longwave radiation~~ (orange triangles).~~. Table 6 gives the associated correlations.

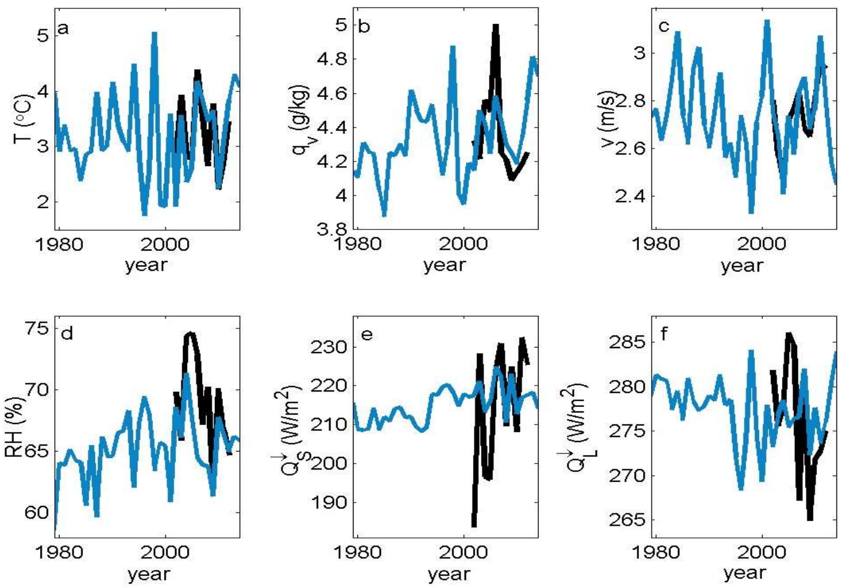

~~**Figure 5**. Mean melt season (MJJAS) weather conditions from the bias-corrected NARR output (blue), 1979-2014, and for the in situ data (black), 2002-2012: (a) temperature, (b) specific humidity, (c) wind speed, (d) relative humidity, (e) incoming shortwave radiation, and (f) incoming longwave radiation.~~

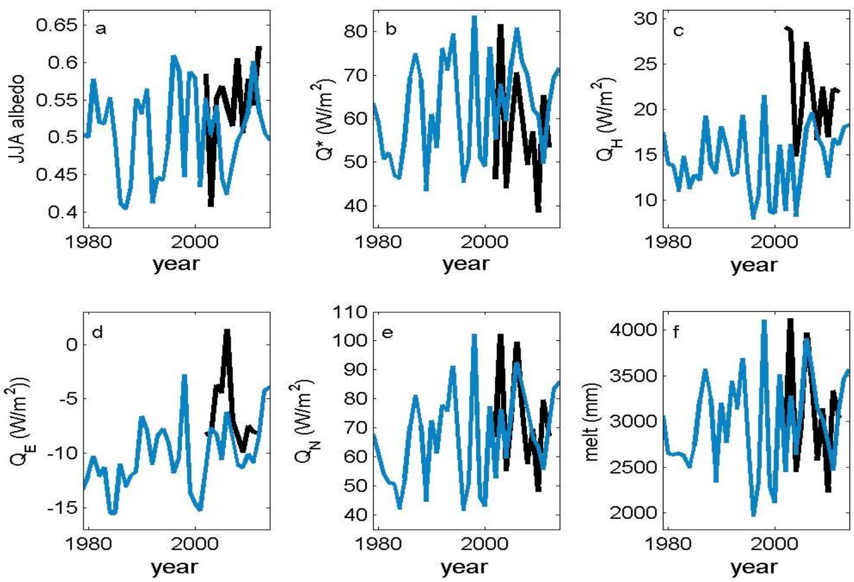

~~**Figure 6**. The evolution of modelled summer surface energy balance and melt from the perturbed NARR output (blue), 1979-2014, and from the in situ data (black), 2002-2012. (a) albedo, (b) net radiation, (c) sensible heat flux, (d) latent heat flux, (e) net energy, and (f) total summer melt (mm). All fields are for MJJAS except for albedo, which is shown for JJA, the main melt season.~~

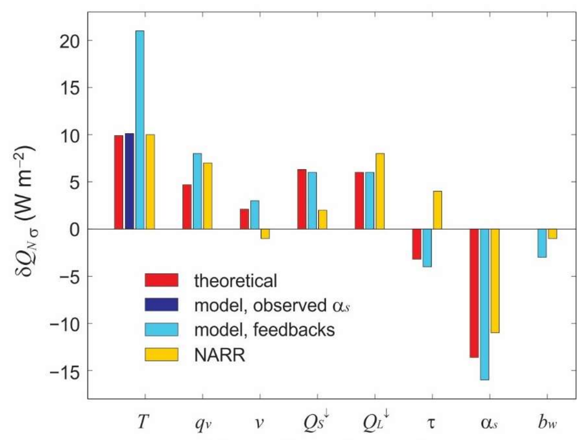

Figure 9. Net energy sensitivity to a 1-σ perturbation in different meteorological variables: comparison of theoretical, *in situ* numerical model, and NARR-based estimates.

Formatted: Font: +Body (Calibri), 11 pt

Formatted: Normal, Left

Formatted: Font: +Body (Calibri), 11 pt